


12-2016

Degradation of high performance polymeric fibers: Effects of sonication, humidity and temperature on poly (p-phenylene terephthalamide) fibers

Nelyan Lopez-Perez
Purdue University

Follow this and additional works at: https://docs.lib.purdue.edu/open_access_theses

 Part of the [Chemical Engineering Commons](#), and the [Materials Science and Engineering Commons](#)

Recommended Citation

Lopez-Perez, Nelyan, "Degradation of high performance polymeric fibers: Effects of sonication, humidity and temperature on poly (p-phenylene terephthalamide) fibers" (2016). *Open Access Theses*. 873.
https://docs.lib.purdue.edu/open_access_theses/873

This document has been made available through Purdue e-Pubs, a service of the Purdue University Libraries. Please contact epubs@purdue.edu for additional information.

**PURDUE UNIVERSITY
GRADUATE SCHOOL
Thesis/Dissertation Acceptance**

This is to certify that the thesis/dissertation prepared

By Nelyan Lopez-Perez

Entitled

DEGRADATION OF HIGH PERFORMANCE POLYMERIC FIBERS: EFFECTS OF SONICATION, HUMIDITY AND TEMPERATURE ON POLY(P-PHENYLENE TEREPHTHALAMIDE) FIBERS

For the degree of Master of Science in Materials Science Engineering

Is approved by the final examining committee:

Dr. John Howarter

Chair

Dr. Kendra Erk

Dr. Carlos Martinez

To the best of my knowledge and as understood by the student in the Thesis/Dissertation Agreement, Publication Delay, and Certification Disclaimer (Graduate School Form 32), this thesis/dissertation adheres to the provisions of Purdue University's "Policy of Integrity in Research" and the use of copyright material.

Approved by Major Professor(s): John Howarter

Approved by: David Bahr

Head of the Departmental Graduate Program

12/7/2016

Date

**DEGRADATION OF HIGH PERFORMANCE POLYMERIC FIBERS: EFFECTS
OF SONICATION, HUMIDITY AND TEMPERATURE ON POLY (P-
PHENYLENE TEREPHTHALAMIDE) FIBERS**

by

Nelyan López Pérez

A Thesis

Submitted to the Faculty of Purdue University

In Partial Fulfillment of the Requirements for the degree of

Master of Science in Materials Engineering



Department of Materials Engineering

West Lafayette, Indiana

December 2016

THE PURDUE UNIVERSITY GRADUATE SCHOOL

STATEMENT OF THESIS APPROVAL

Dr. John Howarter, Chair

Department of Materials Engineering

Dr. Kendra Erk,

Department of Materials Engineering

Dr. Carlos Martínez

Department of Materials Engineering

Approved by:

Dr. David Bahr

Head of Materials Science Engineering Graduate Program

To Adrián David González López, my nephew. I dedicate this work to you, although you might not understand at this moment, since you are only two. I hope that one day you read this and know that you are the product of a family full of love, who have given me the tools, encouragement, inspiration and strength to walk through this rough path called graduate school. I know that they will do the same for you, whatever you choose to do. I have come to understand that huge joy can come in the small and simple things that life brings, like the smile of a child. Your smile has done that for me. Thanks for being a spark of light in some of my toughest times.

And in memory of Gloria Ana Rivera Machado, my grandmother. She was a perfect example of resilience and empowerment. She taught me invaluable life lessons that I will keep forever. I am blessed to have had such a strong and lovely woman as my grandmother.

With all my love,

Nelyan

ACKNOWLEDGEMENTS

I will like to thank Dr. John A. Howarter for his support and advice through this project and choosing me to be a member of his team. I would like to give thanks to all the graduated students and fellow coworkers in Dr. Howarter's team for contributing ideas and feedback on my project. Special thanks to Gamini P. Mendis, for all the training, SEM images, and guidance, and Logan T. Kearney for his help in the sample preparation for tensile testing.

Also, thanks to the now Dr. Shane Peng and Dr. Jairo Díaz for their training and help in the DMA. Thank you all for sharing of your time and knowledge with me.

Thanks to the members of my committee, Dr. Kendra Erk, and Dr. Carlos Martinez for their evaluation and remarks on this thesis.

TABLE OF CONTENTS

LIST OF TABLES.....	vii
LIST OF FIGURES.....	viii
ABSTRACT.....	x
CHAPTER 1: INTRODUCTION.....	1
CHAPTER 2: PROPERTIES OF HIGH PERFORMANCE FIBERS.....	3
2.1 High Performance Fibers Used for Body Armor.....	5
CHAPTER 3: PPTA.....	8
3.1 Fiber Structure.....	10
CHAPTER 4: DEGRADATION OF BALLISTIC FIBERS.....	13
4.1 Characterization Techniques.....	13
4.1.1 Dynamic Mechanical Analysis.....	14
4.1.2 Tensile Testing.....	14
4.1.3 Thermogravimetric Analysis.....	16
CHAPTER 5: SONICATION.....	17
CHAPTER 6: BACKGROUND.....	19
6.1 Humidity and Temperature.....	19
6.2 Effects of Water on PPTA.....	19
6.3 Creep.....	20
6.7 Fracture.....	23
CHAPTER 7: EXPERIMENTAL.....	25
7.1 Sonication and Sample Preparation.....	25
7.2 Dynamic Mechanical Analysis.....	26
7.2.1 Humidity Ramp Test.....	26
7.2.2 Cycle-Humidity Test.....	27
7.2.3 Long Creep Test.....	28
7.3 Humidity Chamber.....	29
7.4 Scanning Electron Microscopy.....	29
7.5 Thermogravimetric Analysis.....	29
7.6 Tensile Testing.....	30

CHAPTER 8: DATA AND DISCUSSION.....	31
8.1 Humidity Ramp Test.....	31
8.2 Cycle-Humidity Test.....	36
8.3 Long Creep Test.....	39
8.4 SEM Images.....	41
8.5 Thermogravimetical Analysis.....	43
8.6 Tensile Testing.....	44
CHAPTER 9: CONCLUSIONS AND FUTURE WORK.....	47
REFERENCES.....	50

LIST OF TABLES

Table		Page
1	List of different chemical and mechanical degradation factors.....	13
2	Mechanical properties of Twaron (PPTA) fibers.....	25
3	Values obtained from the fitting of the long creep test.....	28
4	Properties of the non-polar solvent, hexane.....	39

LIST OF FIGURES

Figure		Page
1	Structure and dimensions of fibers made out of different common materials used for ballistic fibers.....	4
2	Molecular structure of UHMWPE.....	5
3	Molecular structure of PBO.....	6
4	Comparison of specific strength vs. the specific stiffness of commercially available high performance fibers	7
5	Chemical structure of PPTA.....	8
6	Schematic of the dry-jet wet spinning process to form PPTA fibers...	9
7	Intermolecular arrangement of PPTA chains.....	7
8	PPTA sample after TGA test under a temperature ramp to 1000C.....	10
9	Model proposed by Li et al. of the structure of PPTA fibers.....	11
10	Pleated structure proposed by Dobb et al.....	11
11	Pleated structure proposed by Morgan et al.....	12
12	Stress-strain curve of a brittle vs. a plastic semicrystalline material...	15
13	Sketch of PPTA fibers in sonication bath.....	17
14	Stages of creep in a polymer.....	21
15	Example of the data extracted from the DMA and how the amount of creep is calculated	21
16	Sketch of the formation of water layers between PPTA crystallites...	22
17	Different types of fractures in fibers.....	23
18	Crack propagation model proposed by Morgan et al.....	24
19	Segment of the humidity ramp test.....	26
20	Relative humidity steps on the humidity ramp test.....	27
21	Relative humidity steps on the cycle-humidity test.....	27
22	Sketch of the costume made humidity chamber.....	29
23	Fixture used for tensile testing	30
24	Complete humidity ramp test for neat PPTA fiber sample at 30°C....	31
25	Humidity ramp test for neat PPTA fiber sample at 30°C.....	32

26	Humidity ramp test for neat PPTA fiber sample at 60°C.....	32
27	Humidity ramp test of PPTA fibers sonicated for 2 hours at 30°C.....	33
28	Humidity ramp test of PPTA fibers sonicated for 2 hours at 60°C.....	33
29	Humidity ramp test of PPTA fibers sonicated for 6 hours at 30°C.....	34
30	Humidity ramp test of PPTA fibers sonicated for 6 hours at 60°C.....	34
31	Strain percent difference under each condition related to the initial strain percent at 0% RH.....	35
32	Cycle-humidity test for neat PPTA fibers at 30°C.....	36
33	Cycle-humidity test for PPTA fibers sonicated for 2 hours at 30°C...	37
34	Cycle-humidity test for PPTA fibers sonicated for 6 hours at 30°C...	37
35	Comparison of the strain difference of neat and sonicated fibers at 30°C.....	38
36	Prediction of the creep behavior of Neat and sonicated PPTA fibers on polar and non-polar solvents for 2 hours.....	40
37	Prediction of the creep behavior of Neat and sonicated PPTA fibers on polar and non-polar solvents for 2 hours. Normalized strain and logarithmic time scale.....	40
38	Cross sectional image of PPTA fiber yarn.....	42
39	SEM images PPTA fibers sonicated at 2, 4, and 6 hours.....	42
40	Evidence of the presence of kink bands in sonicated PPTA fibers.....	42
41	Example of how TGA data is analyzed.....	43
42	Moisture uptake of sonicated PPTA fibers after sonication and after 24 hours exposed to 30°C and 50%RH.....	44
43	Elastic modulus of neat and sonicated fibers after sonication and 24 hours in the humidity chamber at 30°C and 50%RH.....	45
44	Peak load of neat and sonicated fibers after sonication and 24 hours in the humidity chamber at 30°C and 50%RH.....	44

ABSTRACT

López Pérez Nelyan. M.S. Materials Science and Engineering, Purdue University, December 2016. Degradation of High Performance Polymeric Fibers: Effects of Sonication, Humidity and Temperature on PPTA Fibers. Major Professor: John A. Howarter.

High performance fibers are characterized by properties such as high strength and resistance to chemicals and heat. Due to their outstanding properties, they are used on applications under harsh environments that can degrade and decrease their performance. Fiber degradation due to different chemical and mechanical factors, is a process that begins at a microstructural level. Changes in the polymer's chemical or physical structure can alter their mechanical properties. Knowledge of the structure-properties relationship and the effects of environmental chemical and physical factors over time, is crucial for the improvement and development of high performance fibers.

In this study ballistic fibers of poly(p-phenylene terephthalamide) (PPTA) were studied. Methods of accelerated degradation were used to mimic the weariness of the fibers over long periods of time at a smaller time range. Fibers were subjected to ultrasonication in aqueous solution at pH 7 for up to six hours in order to produce surface damage. Once degraded, properties like the creep behavior of these fibers were studied under a humidity range of 0-80% and temperatures of 30°C and 60°C. Characterization of the chemical and mechanical properties of degraded PPTA fibers were characterized by thermogravimetric analysis (TGA), dynamic mechanical analysis (DMA), scanning electron microscopy (SEM), and tensile testing to failure.

Sonication produces small but significant changes in the crystalline structure of the fibers that allows the formation of layers of water and consequently affecting mechanical properties like the elastic modulus and peak load. These small changes can be related to the early stages of degradation. Moreover, this study shows the efficiency of techniques such as the DMA for the detection of early signs of degradation by measuring the amount of creep the material undergoes as humidity changes.

CHAPTER 1: INTRODUCTION

Degradation is the process at which a material loses its performance over time. Usually it is known that a material is degraded when it fails during service. However, this process starts with small changes in the material's physical and chemical structure. For example, changes in the crystallinity or bond breaking are some of the slight degradation steps that take place at an early stage in the process and their effects are magnified with time and continuous exposure to the environment.

The aim of this project is to study the nanostructural degradation process in high performance polymer fibers that are used for body armors. These fibers are characterized for having outstanding properties such as high elastic modulus, chemical and thermal resistance, and possess high crystallinity. All of these properties are attributed to their chemical composition and physical structure. Any alteration in the order of the composition and structure of the fibers may affect their chemical and mechanical properties. This implies that said changes affect the performance of the material, which sometimes results loss of the mechanical properties and consequently, failure during service. This is of great concern for users of soft body armors, since it represents a risk of death or serious injury. Chemical and physical factors in the environment such as high temperatures, humidity, low and high pH found in sweat, and wear can alter the material at the molecular level and display their effects as a reduction of the material's performance at larger scales. Hence, studying the early stages of the degradation process of these high performance fibers is important to predict and prevent their failure while in service.

To study the degradation process of high performance fibers under normal use conditions can take years. Therefore, various methods to accelerate the degradation can be employed in order to enable the study of this process at a laboratory setting and reduced timescale while mimicking the real use conditions. One of the methods used for the degradation of fibers is sonication, which can alter the order and crystallinity of materials due to vibrations, heat and pressure differences between the material and the media it is submerged in. In this project, sonication is used as counterpart method of degradation that accelerates said process due to the localized differences in pressure and temperature as sonication takes place. The former can be seen as an analogue to the effects of folding and

wear, whereas the latter can be related to thermal degradation due to body heat, temperature during service and storage settings. More details about sonication and its effects on fibers are discussed in section 5.

High performance fibers like those made out of poly(p-phenylene terephthalamide) (PPTA) are one of the most commonly used fibers for body armors and the main subject of our study. This project focuses on the detection of early degradation signs on PPTA fibers through sonication. In addition, the goal is to determine the effectiveness of mechanical testing as an approach to determine early and small signs of degradation. Changes in the modulus and the tensile strength of the fibers are the properties measured with these mechanical testing methods. Although changes can be small they can be used to predict further changes in the performance of the fibers for a wider range of time.

CHAPTER 2: PROPERTIES OF HIGH PERFORMANCE FIBERS

Fibers are materials that can be used for a wide variety of applications from clothing to tension cords and bullet proof vests. These materials can be engineered to be useful for specific needs. There are two groups of fibers: natural and synthetic. Natural fibers such as cotton, wool, silk, and hemp are obtained from vegetable sources or from the hair and proteins of animals. On the other hand, synthetic fibers are produced from molecular organic or inorganic sources.

Some synthetic fibers are composed of polymers, which are drawn to align the polymer chains in the same direction. The purpose of the drawing process is to increase the aspect ratio of the material. We refer to the aspect ratio as the length of the material divided by its diameter¹. Fibers possess high aspect ratios (100-500), which means that their diameter is very small when compared to their length¹. Some polymeric fibers that take this property to their advantage are **high performance fibers**. This group of fibers possess at least one superior physical, mechanical and chemical property². They are usually distinguished for possessing high yield stress, elastic modulus, ductility, thermal, impact and chemical resistance. However, it is difficult to obtain a material that offers all these properties simultaneously³. Therefore, a great amount of research is involved in developing and improving high performance fibers to develop the next generation of body armor.

The superior properties that high performance fibers possess are attributed to the chemical and physical structure of the polymer. The chemical composition and the tacticity (how the side are arranged along the polymer chain⁴) govern the material's ability to form secondary bonds and crystalline regions respectively. Consequently, this dependence on the structure and chemical composition of the polymers affect the performance of the final product at macroscale. Chemically, polymers used for the production of ballistic fibers often have strong covalent bonding on the backbone, should be linear - to enable chain folding and obtain higher crystallinity- and must be able to acquire an "extended chain" structure⁵. **Figure 1**, shows a schematic of different fibers, including some used for high performance applications. The figure details the different structures of the fibers made from extended polymer chains and their size scales^{6,7}. Fibers like Kevlar and Spectra [trade names for poly(p- phenylene terephthalamide) and ultra high molecular weight polyethylene

respectively] are composed of macrofibrils and each microfibril is formed by the extended polymer molecules that possess diameter of 0.5-1 nm.

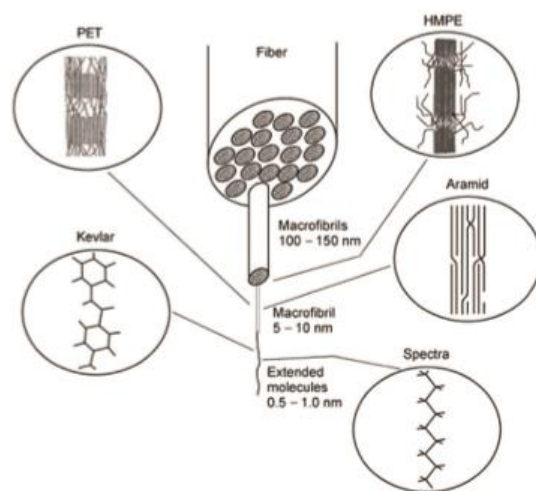


Figure 1. Structure and dimensions of fibers made out of different common materials used for ballistic fibers^{6,7}.

Other factors that contribute to the performance of these fibers is the spinning and drawing process, at which the polymer molecules are aligned to produce the fibers. Two of the most common spinning processes are: melt and solution spinning. Melt spinning consists in heating and extruding the polymer without the use of a solvent. This process is recommended for polymers that have a broad range of temperatures at which the viscosity is the adequate for extrusion and degradation does not take place. On the other hand, solution spinning does require the use of a solvent because the polymer cannot be melt extruded. Under this category, there are two other subcategories that are based on the removal of the solvent: dry and wet spinning. In the case of dry spinning, the solvent is removed by evaporation, while in wet spinning the solvent is removed with another solvent in what is known as a coagulation bath². Degradation can be induced during the production the fibers due to the high temperatures and residues of the solvent used at this stage. At high temperatures the material is more prone to oxidation, which can lead to the release of free radicals and later on, chain scission. Another example of the effects of spinning processes is the formation of microvoids due to the evaporation of the solvent once the product is finished, which can affect the performance of the fiber while in use⁸. Section 3 will discuss the spinning process for PPTA fibers in more detail.

2.1 High performance fibers used for body armor

The use of high performance fibers for soft body armors is relatively new (being developed in the mid-20th century). Before the synthesis of advanced materials like PPTA fibers, Nylon and silk fibers were used for the development of body armors⁹. Yet, there was a necessity of lightweight and flexible body armors that offered more protection than the offered by previously used fibers. The first commercially developed ballistic fiber was Kevlar developed by DuPont in the 1960's but available in the market in 1971^{9,10}. Kevlar is made out of poly(p-phenylene terephthalamide) and it is discussed more broadly in section 3. After the successful development and commercialization of Kevlar, other polymeric fibers have been produced for body armors.

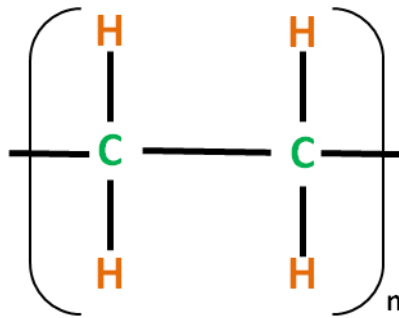


Figure 2. Molecular structure of ultra high molecular weight polyethylene (UHMWPE).

An example of other polymers used for the production of ballistic fibers is ultra-high molecular weight polyethylene (UHMWPE), commercially known as Dyneema or Spectra (**figure 2**). This type of polyethylene has a weight average molecular weight of around two million which means that each chain has an approximate length of around 10 microns¹¹. Polyethylene is chosen for this application due to its flexibility, low density, and high crystallinity, strength and fatigue resistance¹². Drawing UHMWPE increases its crystallinity and takes advantage of the strong covalent forces that govern the chain structure by aligning the polymer backbone in the direction of the applied force, and increases interchain connectivity¹¹. Although UHMWPE is commonly used for ballistic applications, some of its disadvantages originate from its low melting temperature. UHMWPE can exhibit creep behavior at room temperature and, it is accelerated at

temperatures above 150°C¹¹. Therefore, the use of UHMWPE is limited to a small range of service temperatures.

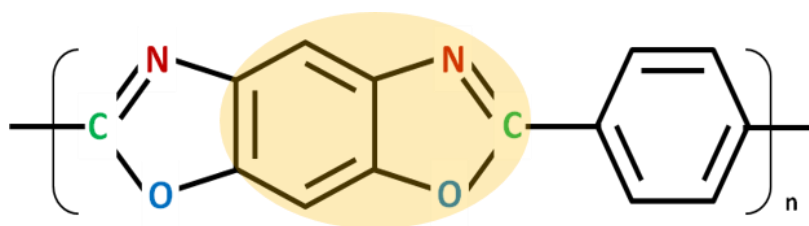


Figure 3. Molecular structure of PBO. The highlighted region indicates the benzoxazole ring.

Another polymer used for ballistic purposes is poly(p-phenylene-2,6-benzobisoxazole) (PBO), commercially known as Zylon in its fiber form. The chemical structure of this polymer consisting in aromatic rings (see **figure 3**) gave the material higher rigidity. Fibers made out of PBO can reach an elastic modulus of 360 GPa, making it the highest among the fibers used for ballistic materials (Twaron PPTA fibers have an elastic modulus ranging from 60-120GPa¹³, and UHMWPE has an elastic modulus of approximately 115GPa¹¹)¹⁴. However, it has been found that factors such as exposure to ultraviolet radiation (UV), and high and low pH this material affect the stability of the benzoxazole ring in its molecular structure¹⁵. The instability of the benzoxazole ring was one of the factors studied after a body armor vest failed during service. This incident prompted a series of investigations to understand the failure of PBO fibers. The failure of these fibers was due to presence of phosphoric acid that was residue of the manufacturing process¹⁵. When PBO fibers are in contact with humidity and high temperatures a reduction in the average molar mass of the polymer and the tensile strength of fibers has been measured. These results are evidence that a hydrolysis reaction among the chains takes place¹⁶. Hydrolysis leads to chain scission and premature failure.

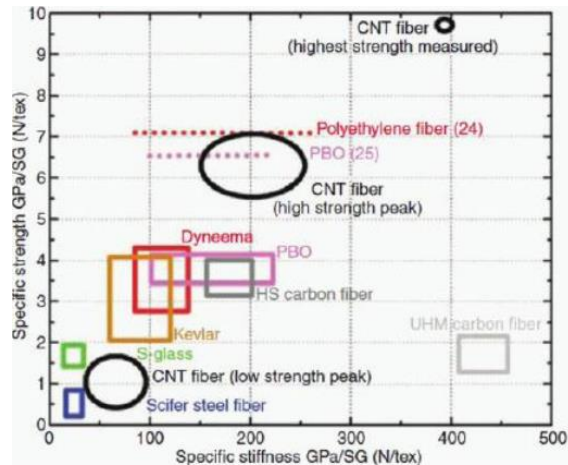


Figure 4. Comparison of the specific strength versus the specific stiffness of commercially available high performance fibers⁹.

The ultimate goal of high performance fibers used for soft body armors, like the previously mentioned, is to offer ballistic protection without compromising weight and comfort¹⁷. **Figure 4** shows a graph of different fibers that are commercially available for ballistic applications⁹. The graph compares the material's specific strength versus its specific stiffness (modulus). These "specific" properties refer to the value of the fiber's modulus or strength respectively, divided by its density¹⁸. According to **figure 4** the strongest fibers available are those made out of carbon nanotubes (CNT) but they are also the stiffest, making them more brittle. On the other hand, ballistic fibers like Kevlar, Dyneema and PBO are in the range of 50-225 GPa/SG specific stiffness and 2-4.50 GPa/SG specific strength. They are less strong and stiff than CNTs, because although they possess high crystallinity they are not as crystalline as CNTs, therefore, they show some elasticity and exhibit more flexibility.

Despite the values of properties such as stiffness and strength of these materials, one single fiber does not offer enough coverage for ballistic protection. These fibers are bundled into yarns that are formed into woven textiles. These woven textiles sheets or panels are arranged on top of each other in different directions to create the fully packed armor.

CHAPTER 3: POLY (P-PHENYLENE TEREPHTHALAMIDE)

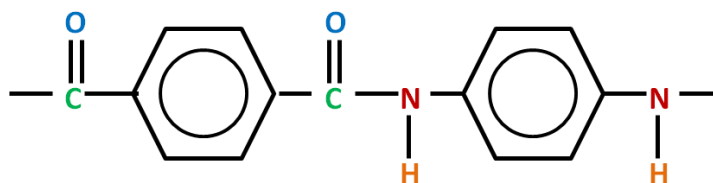


Figure 5. Chemical structure of poly(p-phenylene terephthalamide) (PPTA). PPTA is the polymer used to produce commercially known high performance fibers such as Kevlar and Twaron.

Poly(p-phenylene terephthalamide) (PPTA) is an aramid polymer, which means it is composed of aromatic rings and amide functional groups. Its repeat unit is a byproduct of the condensation reaction of para-phenylene diamine with terephthaloyl chloride to obtain the chemical structure showed in **figure 5**. The resulting molecule is stable due to the presence of aromatic rings in the backbone. The stiffness of the chains is attributed by the para position of the aromatic rings, while its crystallinity is enabled by the presence of amide groups in the lateral direction. The latter permits hydrogen bonding and chain packing¹⁹.

The rigidity of the PPTA chains make the material difficult to process. However, PPTA can be dissolved in solvents such as H_2SO_4 , HF and methasulfonic acid¹⁷. When the polymer is combined with one of these solvents, a liquid crystal system is produced. A liquid crystalline polymer (LCP) shows properties of liquids and crystals. LCPs have mesogenic regions, which can form crystalline phases²⁰. Polymers that acquire a liquid crystal behavior when a solvent is added, like PPTA, are considered a lyotropic systems²¹. PPTA degrades at temperatures below its melting point, therefore processing PPTA under a lyotropic condition prevents degradation due to high temperatures²⁰. Another benefit that this processing technique provides is that dry-jet wet spinning process is possible and results in radial crystalline orientation¹⁹.

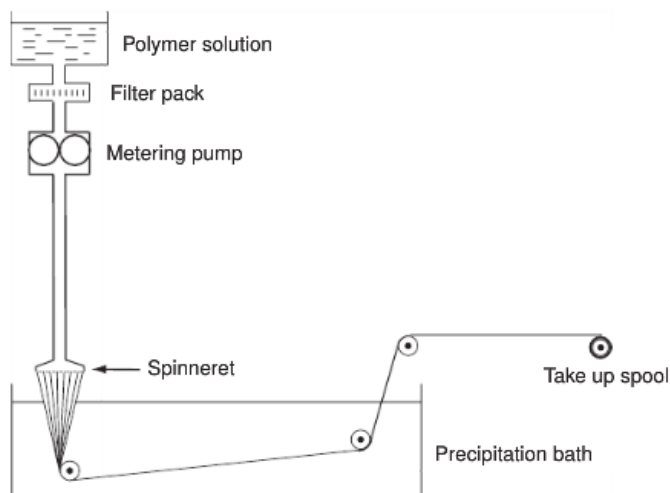


Figure 6. Schematic of the dry-jet wet spinning process to form PPTA fibers².

In the dry-jet wet spinning process (**figure 6**), the lyotropic PPTA solution (20% solvent, 80% polymer) is passed through the spinneret holes to form the filaments (fibers). After this stage the filaments are drawn a certain distance (0.5-1cm) until it reaches the next stage which is the coagulation bath². This stage consists in submerging the PPTA filaments in a water bath at 0°C-5°C to remove the solvent. The following step is a heat treatment at high temperature (550°C) but only a few second to further align the polymer chains². This process enables the ability of PPTA molecules to form hydrogen bonds (see **figure 7**), and the characteristic high crystallinity of these fibers.

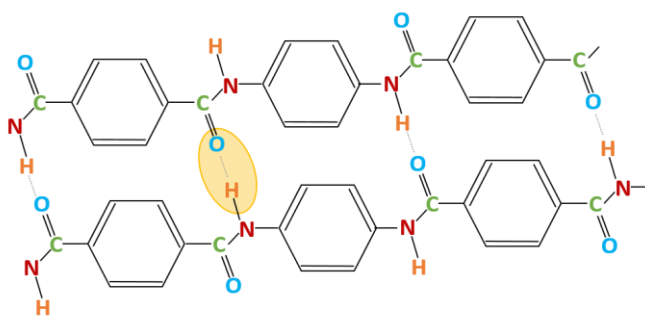


Figure 7. Intermolecular arrangement of PPTA chains. Chains are held together by hydrogen bonding, as marked by the highlighted area on the sketch.

Once the PPTA polymer is transformed into fibers, consequences in the melting temperature occur. In the fiber form, PPTA degrades at around 500°C but does not melt as

the temperature continues to raise. **Figure 8** shows a fiber sample after it has been heated up to 1000°C. The sample is practically char, nonetheless it never transitions to a liquid state. Hence, the fiber structure enhances the physical and chemical properties such as increasing the elastic modulus due to more crystallinity and increasing the thermal resistance due to the strong bonds between and stability among the molecules.

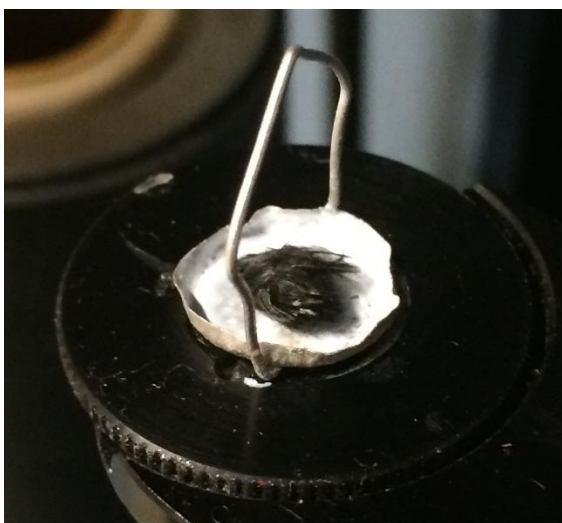


Figure 8. PPTA fiber sample after thermogravimetric analysis test under a temperature ramp to 1000°C. The sample does not melt but degrades and all that is left is char.

3.1 Fiber structure

There are several models that describe the structure of PPTA fibers. However, the consensus model is that the structure of these fibers is formed by a skin barrier (on the surface) and a core. This skin-core arrangement is created at the coagulation stage of the dry-jet wet spinning process⁶. As the PPTA LCP system is drawn through this process, the chains located closer to the surface are immediately aligned while those at the center are “relaxed”⁶. Consequently, the core is formed by imperfectly packed but ordered chains and differs from the skin structure in density, amount of void and orientation of the fibrils^{6,22,23}. **Figure 9** demonstrates a model proposed by Li et al, which explains the differences between the core and skin structures^{24,25} and the overall radial structure of the fiber.

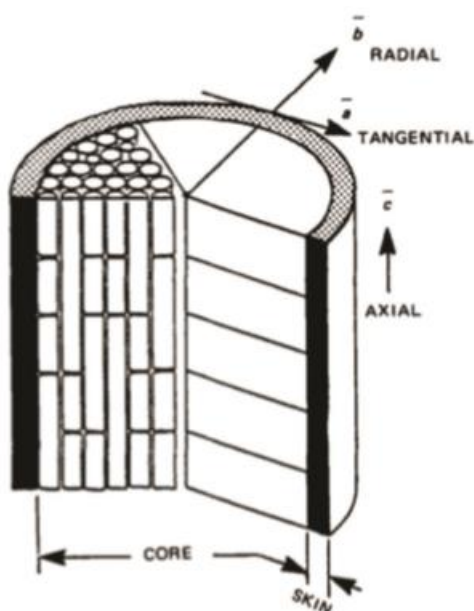


Figure 9. Model proposed by Li et al. of the structure of PPTA fibers. In it, there is a skin barrier at the surface and a core formed of crystallites that grow radially. The crystallites are packed in cylinders that are aligned to the drawing axis^{6,24,25}.

Another physical characteristic of PPTA fibers is their pleated structure as seen in **Figure 10** proposed by Dobb et al. In this model the oriented crystals are located parallel to each other and in a way that the intermolecular hydrogen bonding is perpendicular to the fiber's surface^{6,26}. X-ray diffraction results show that the pleated structure is formed by (200) planes that create two alternating sets of sheets that have a periodicity of 250 and 500nm⁶. A 170° angle between the two sheet surfaces that form the pleated structure^{6,26}.

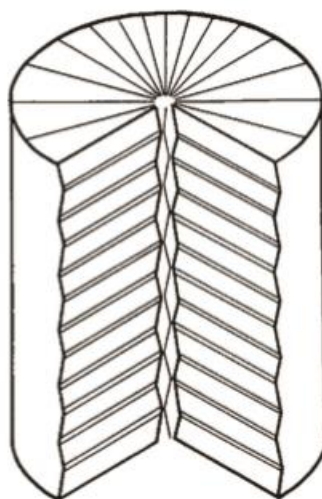


Figure 10. Pleated structure proposed by Dobb et al²⁶.

As the dry-jet wet-spinning process continues and enters the solidification phase, chain-end defects are induced in PPTA fibers. **Figure 11** shows a schematic of this structure proposed by Morgan et al. In said model the core consists of fibrils²⁷.

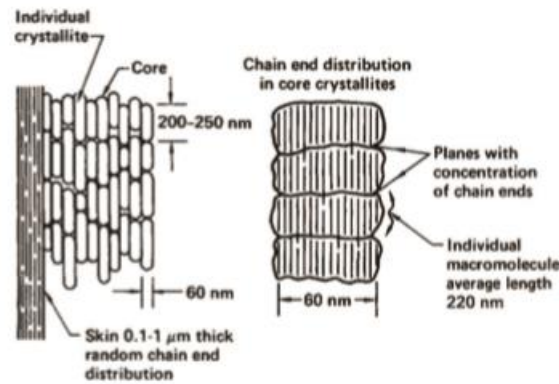


Figure 11. Pleated structure proposed by Morgan et al²⁷. This structure is similar to the one found in **figure 9** but it is more specific in the dimensions of the skin-core morphology. It also concludes that the diameter of the fibrils is around 60nm.

CHAPTER 4: DEGRADATION OF BALLISTIC FIBERS

Table 1 presents a variety of chemical and mechanical degradation factors relevant to ballistic fibers. Degradation will first take place in the most susceptible (weaker) bonds on the polymer chain. Hence, to degrade a polymer chain, the degradation factor must provide the sufficient energy to break those bonds. This can result in one of two pathways: chain scission or crosslinking. Either of them has consequences on the performance of the material. For example, cross-linking increases the molecular weight and the viscosity of the polymer, while chain scission has the opposite effect²⁸.

Chemical	Mechanical
Exposure to Radiation (UV, sunlight)	Fatigue
Humidity	Compression
Temperature	Tension
pH / redox reactions	Shear
Chemical attacks (such as solvents and sweat)	

Table 1. List of different chemical and mechanical degradation factors.

4.1 Characterization Techniques

Signs of degradation on materials, like changes in color, are visible at first sight. However, degradation small changes in the chemical and physical structure of the materials sometimes are not visible but do have an effect on the performance of the fibers. Hence, chemical and mechanical characterization techniques are employed to study these small changes and relate the environmental conditions that the materials are exposed to, to the resulting mechanical properties. There are many characterization techniques that detect these changes. For example, chemical degradation can be studied by using methods such as Fourier transform infrared spectroscopy (FTIR) which detects any changes in the vibration of the functional groups conforming the polymer chains. However, physical degradation can have more visible signs that can be seen through microscopy methods. Fibers that have been exposed to different mechanical degradations may exhibit evidence

of kink bands and/or fibrillation. Kink bands are deformation structures that usually appear when fibers like PPTA experience compression or bending, causing a change in the orientation of the polymer chains²⁹. Axial compression weakens the fibers and can lead to their failure³⁰. On the other hand, fibrillation is the separation of the fibrils of a fiber.

These signs of degradation can be detected by microscopy methods such as the scanning electron microscopy (SEM), which is one of the methods employed in this project. Nevertheless, some modes of degradation cannot be visible through these methods but can be detected using mechanical testing methods such as the dynamical mechanical analysis (DMA) and tensile testing to failure. Both of the latter are core measurement methods for this project and will be described in the following sections.

4.1.1 Dynamic Mechanical Analysis

In general, dynamic mechanical analysis (DMA) is a technique that measures the response of a material to an applied force (stress)³¹. Data obtained from this kind of analysis offer information of visco-elastic transitions, damping modulus, and other properties of a material³¹. One of the properties that can be studied using this technique is the material's creep behavior. Creep is the deformation of a material over time when a constant stress is applied, which is essential information to know the range of temperatures at which the material can be used³².

4.1.2 Tensile testing

Tensile testing is a very straight forward characterization technique through mechanical properties of a material can be acquired. Through this method, a stress versus strain curve (**figure 12**) of the material is plotted as the sample under study is stretched in one direction³³. The results of the plotted stress-strain curve show how much elastic and plastic deformation the material undergoes until it fails and breaks. Ductile materials like the semicrystalline material represented in red in **figure 12**, have an initial elastic response. This means that if the applied load is removed, little to no deformation is done. If the material is stretched even further, it will reach a point where plastic deformation takes place known as the yield point. In the case that the material is stretched even more, it will reach its ultimate tensile strength. This point indicates the maximum load that the material can

support without breaking³⁴. After reaching this point, a semicrystalline material will experience a wider amount of strain at a lower stress than the ultimate tensile strength. Later on the stress will increase at a higher rate until it the material breaks and fails.

Ballistic fibers possess high crystallinity and will exhibit a brittle behavior such as the green plot in **figure 12**. In this case, the ultimate tensile strength and the fracture point are the same. This is one of the properties that are measured in this project along with the elastic modulus. The latter is determined with the slope of the stress-strain curve.

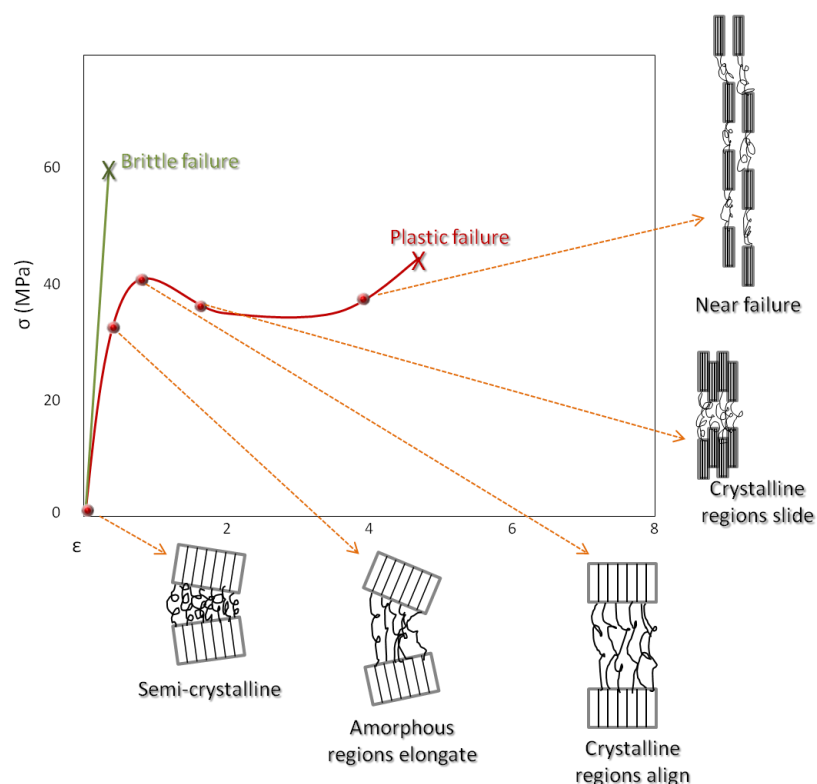


Figure 12. Stress-strain curve of a brittle material versus a plastic semicrystalline material. Effects on the microstructure of the semicrystalline material is shown step by step as it is deformed. This figure is adapted from³⁴: Callister, W. D. *Materials Science and Engineering : An Introduction*; John Wiley & Sons, Inc., 2007.

Tensile testing has been previously used by Obaid et al., to study the effects of environmental conditioning such as alterations on temperature and amount of time exposed to water on high performance fibers³⁵. This study concentrated in aramid fibers and focused in measuring the retention of the values of the mechanical properties through tensile

testing. The data showed that aramid fibers like Kevlar and Twaron retained 100% of their modulus, but had a decrease on their strength (only 42% and 66% retained respectively) and strain at failure (45% and 77% retained) when tested in water at 100°C. Said results substantiate the capability of tensile testing to detect degradation by measuring changes in the mechanical properties of high performance fibers.

4.1.3 Thermogravimetric Analysis

Thermogravimetric analysis (TGA) measures a material's weight loss as it is heated up. This technique offers information of crucial transitions such as the degradation temperature of PPTA fibers and the amount of water retained by the material. Data obtained through this method, is related to the structure of the material, therefore, changes in the crystallinity of the material will be reflected in the data. TGA experiments can be conducted under nitrogen or air environments. The latter can offer information of the oxidation of the material.

The effectiveness of TGA as a characterization method for high performance fibers has been proven before. A study conducted by Liu and Yu, used TGA to compare and evaluate the thermal stability of different high performance fibers such as PBO, PPTA and UHMWPE among other fibers composed made out of copolymers³⁶. Results revealed that PBO has a higher thermal stability than PPTA fibers (like Kevlar and Twaron), and UHMWPE has the lowest thermal stability. These conclusions are the same for both air and nitrogen atmospheres. Other studies by Perepelkin et al. used TGA for the determination of the thermal resistance of different para-aramid fibers³⁷. Results show that thermooxidation is crucial at temperatures above 450 to 500°C and that 4% of the fiber's weight is lost at temperatures ranging above 490-500°C. Information obtained through these studies can be used to set a range of service temperatures and are an example of the relevance of TGA data.

CHAPTER 5: SONICATION

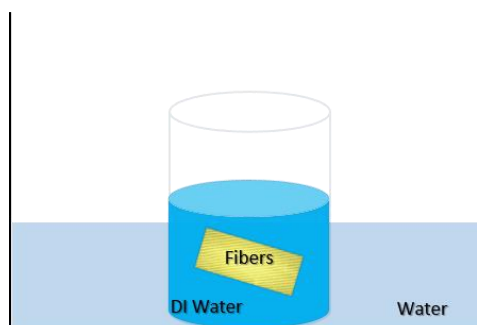


Figure 13. Sketch of PPTA fibers in a sonication bath.

Due to the degradation effects of sonication in polymeric materials like fibers, it can be used as a method for accelerated degradation. This method may induce similar fatigue conditions, such as other methods that involve the folding of PPTA fibers. A research team at the National Institute of Standards and Technology have developed a costume made machine that folds body armor panels (woven material used as a protective layer in soft body armors) cyclically^{38,39} to replicate the effects of wear. However, due to the harsh environment that ultrasonic waves create when they travel through a liquid media, it can be used to simulate the same effects as the folding machine developed at NIST.

Ultrasonic waves are produced at a range of 20kHz and above⁴⁰. Sonication at this frequency is commonly used for cleaning, welding, emulsifying, and to accelerate chemical reactions like polymerization and polymer degradation^{40,41}. In an ultrasonic bath (as seen in **figure 13**), ultrasonic waves travel through a liquid media. Due to the motion of the liquid molecules at high frequencies, an increase on temperature and the formation of bubbles is produced. Moreover, pressure differences are generated through the medium where high and low pressure areas perform compression and rarefaction/extension respectively on the material that is immersed in the medium⁴². These phenomena affect the material that is exposed to sonication both in the surface and the internal structure of the fibers. Consequences like the generation of shock waves and microstreaming jets that are produced when bubbles expand and collapse, can lead to intermolecular tearing and the

liberation of free radicals on materials like fibers^{41,42,43}. Polymer degradation caused by sonication usually do not produce any chemical changes, but may cause the breaking of chemical bonds, which can lead to a reduction in molecular weight⁴⁴.

One of the parameters that determine the rate of degradation of a material as it is sonicated is the solvent that is used as the media. Therefore, the solubility parameter of the solvent and the polymeric material is essential for the degradation process⁴⁵. Polymer degradation due to sonication is usually measured by detecting changes in the molecular weight distribution of the polymers⁴⁴. However, ballistic fibers like PPTA, are highly resistant to solvents, therefore the weight distributions is difficult to obtain. Also, the use of highly abrasive solvents, such as sulfuric and hydrofluoric acid, are not commonly present when the material is used for ballistic protection purposes. Therefore, the use of said solvents would not mimic the degradation of PPTA fibers under normal use conditions, and hence will add additional and unnecessary degradation. Nevertheless, testing of the mechanical properties of the fibers can also give a quantitative measurement of the material's degradation.

Aging studies on polymeric membranes have been carried using sonication as a method for accelerated degradation. The results conclude that sonication increases the pore radius, density and porosity of membranes⁴¹. Some of the consequences these changes produce are the formation of cracks in the material which increase the permeability. This is an example of how sonication can affect both the structure and the performance of the polymeric material.

Sonication has been said to reduce the effects of ultraviolet (UV) degradation on PPTA fibers and also increase their strength⁴⁶. Andrassy et al. address the improvement on the mechanical properties to ordering of the fiber structure and the formation of crosslinks⁴⁶. These results do not show any chemical evidence of crosslinking nor take in consideration the effects of moisture in the fibers. Other studies revealed the effects of sonication on PPTA fibers by obtaining visual evidence of degradation such as kink bands and fibrillation⁴⁷. However, no information of the changes on the mechanical properties was provided.

CHAPTER 6: BACKGROUND

Previous studies have revealed the physical effects of sonication on PPTA fibers which include the formation of kink bands, and fibrillation⁴⁷. Others have gone further in these studies and concluded that submitting PPTA fibers to sonication treatment can help improve their strength and prevent degradation due to UV exposure⁴⁶. The latter is attributed to the possible “crosslinking” of the chains, but no chemical information is offered. The question that raises out of these previous research is if sonication can really improve the strength of PPTA fiber, by reducing the magnitude of the degradation over time. It seems contradictory that effects such as fibrillation can make the material stronger.

Moreover, this project focuses on the effects of ultra-sonication of PPTA fibers and its effects on its mechanical properties at different temperatures and relative humidity. The changes in the mechanical properties were mainly measured by carrying experiments with the dynamic mechanical analysis (DMA) and tensile testing techniques. With this we can obtain information of the material’s mechanical properties such as its elastic modulus and creep behavior under different fibers and the contributions (benefits/disadvantages) of sonication to them.

6.1 Humidity and Temperature

In this project PPTA were exposed to different amounts of relative humidity. Relative humidity (RH) is defined as the amount of water vapor in a volume, with 100% being the saturation point of water in air. It is expressed as a percentage. There is also a difference between the temperature and the apparent temperature. The apparent temperature is perceived temperature as a product of the actual temperature and the relative humidity. Increasing the amount of water vapor, in other words, increasing the relative humidity raises the apparent temperature. Only RH and actual temperature are reported in this project.

6.2 Effects of water on PPTA

It is crucial to understand the reactions of water on PPTA fibers at short and long periods of time for it will determine the life of use of soft body armors⁴⁸. Moreover, water is present in common scenarios like humidity in the environment and sweat from the user. It

is known that moisture is retained in the amorphous regions of the polymer, however, PPTA fibers are characterized by their high crystallinity. This raised the question on how is it possible for these fibers to retain water. Some studies attribute the moisture uptake in PPTA fibers to the polarity of amide groups present in the polymer chains, the presence of microvoids in the surface and hydrophilic salts that are residue of the manufacturing process⁴⁹.

There are models that explain this moisture uptake by a diffusion process between the skin and core structures in the fibers. However, another model called the intercalation model has been proposed. The latter establishes that water penetrates the surface layers of the crystallites⁵⁰. The effects of water on the creep behavior of PPTA fibers is discussed in the following section (6.2).

6.3 Creep

One of the mechanical characteristics that were studied in this project was the creep behavior of PPTA fibers that were subjected to different amounts of sonication time and humidity. Creep is experienced by a polymeric material when it is subjected to constant stress. Under this condition, the strain of the material changes over time as showed in **figure 14**. The creep behavior curve described by the figure is divided in three stages: primary, secondary and tertiary. The primary stage of creep is characterized by a high strain rate until it reaches a constant strain²⁰. Later on, the material enters the secondary creep stage where the strain rate is constant. At the tertiary creep stage the strain rate increases again and leads to fracture. As it is represented in the figure, fracture does not occur instantly, it can occur in minutes or years. Furthermore, the creep behavior of the material is dependent on factors like the temperature and the applied stress. It is expected that the fracture of the polymeric material occurs at shorter amounts of time if these factors (temperature and stress) are increased³². This project is focused on studying the primary creep stage through the DMA technique.

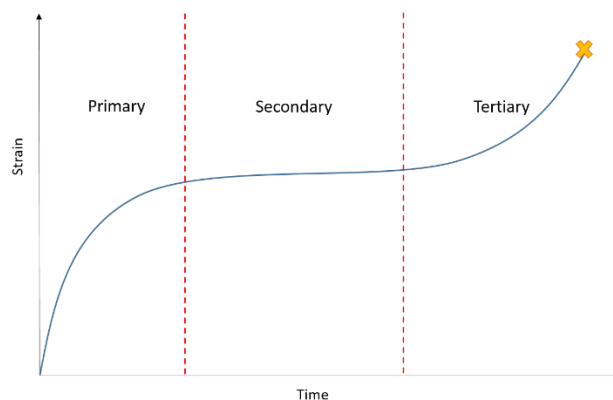


Figure 14. Stages of creep in a polymer.

Figure 15 shows an excerpt of the data obtained from the DMA experiments explained in greater detail in sections 7.2.1 and 7.2.2. This portion of the data, corresponds to the stage at which the sample is under a constant tensile stress (18 N), therefore, it experiences creep. On the x axis, the time is plotted while the y-axis determines the amount of strain (in percentage) the sample undergoes. This experiments consist in submitting the sample to creep at different relative humidity values. Therefore, the final amount of creep will depend not only of the temperature and humidity conditions, but also the creep history. To know the amount of creep the sample has experienced, the difference in strain is calculated based on the initial strain on the creep stage at 0%RH. The initial and final strain are marked on **figure 15** with a green and a red dot respectively. To calculate the strain percent at each of the humidity values, the final value (red dot in **figure 15**) is subtracted to the value of the strain at 0%RH.

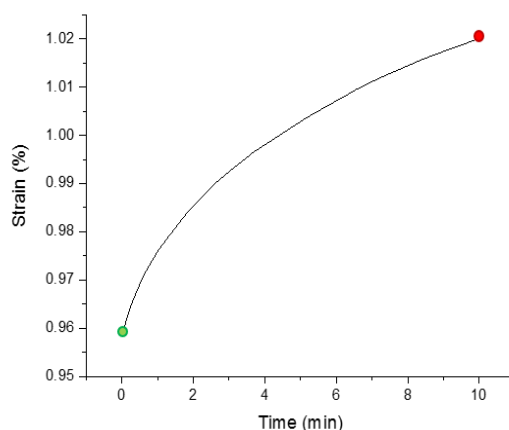


Figure 15. Example of the data extracted from the DMA and how the amount of creep is calculated.

Moreover, polymeric materials like PPPTA fiber, experience nonlinear creep. This behavior has been previously described and modeled with the following power law equation⁵¹:

$$\varepsilon(t) = \varepsilon_0 + mt^n$$

In said equation ε_0 is the initial overall strain (when $t=0$) of the material and n is a parameter intrinsic of the material. With this equation the results from a short creep experiment can be fitted and the values obtained from said fitting allows the prediction of the creep behavior at longer times.

One of the main pillars of this investigation is to understand how sonication of PPTA fibers changes their structure and water adsorption capacity. The amount of water retained in the fibers has affects their creep behavior. It has been previously established by Wang et al., that water molecules form layers between the crystallites⁵². The presence of the water molecules enables the formation of hydrogen bonding. Furthermore, the strength of these bonding forces decreases as the amount of water layers increases. Wang et al. also concluded that at low relative humidity the creep activation energy is higher than at high relative humidity percentages⁵². This means that creep is more likely to occur more rapidly when there is more water, due to the weakening of the hydrogen bonds between the water layers. **Figure 16** demonstrates the formation of the water layers (comparing a monolayer versus a multilayer scenario).

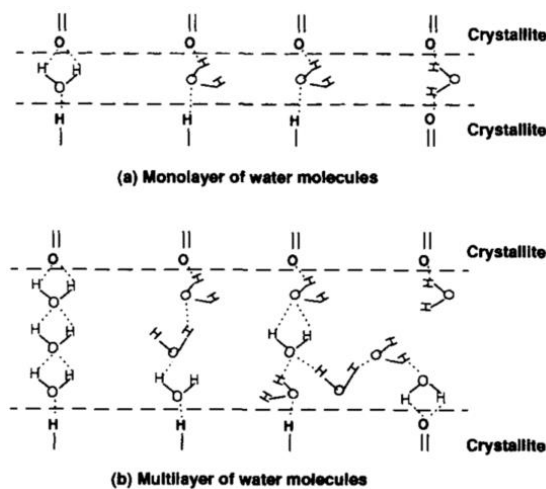


Figure 16. Sketch of the formation of water layers between the PPTA crystallites⁵².

6.4 Fracture

Ballistic fibers such as those made of PPTA have a brittle response when subjected to a tensile load. This is due to the high orientation of the polymer chains and crystallinity. Fracture of these fibers mainly consist of chain-scission⁵³ caused by the chain-end defects mentioned in section 3.1. Said defects do not only affect the failure, but also contribute to the deformation and strength of the fibers^{6,27}. Fracture in highly oriented fibers like PPTA occur by crack propagation that produce an axial split break⁵⁴. These fibers, as mentioned in previous sections, have a higher molecular strength in the axis in which the fiber was drawn than between the molecules. **Figure 17** shows the most common types of fracture found in fibers (axial split can be found in **figure 17.6**)



Figure 17. Different types of fractures in fibers. Group A- Tensile breaks: (1) brittle, (2) ductile, (2a) light-degraded, (3) high-speed mushroom, (4) axial splits, (5) granular, (6) fibrillar, (7) stake-and-socket. Group B-Fatigue: (8) strip and tail, (9) kink bands, (10-11) splits, (12) wear, (13) peeling, (14) rounding. Group C-Others: (15) mangled, (16) cut, (17) melted, (18) natural end of cotton fiber. This figure was taken from⁵⁴.

Failure in PPTA fibers mainly consists in crack propagation. Cracks are formed as a consequence of the breakage of hydrogen bonds between the chains as the fiber experiences tension. In the core, the propagation follows a transverse path along the sites where there are chain ends²⁷. As it reaches the skin, the path follows a transversal and lateral propagation marked by the difference in the structure between the two areas as seen in **figure 18**.

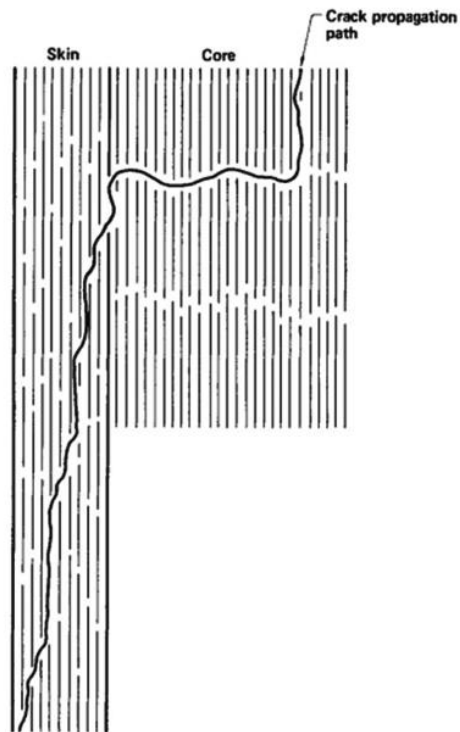


Figure 18. Crack propagation model proposed by Morgan et al^{27,6}.

CHAPTER 7: EXPERIMENTAL

7.1 Sonication and sample preparation

PPTA woven fibers (Twaron, provided by Teijin) were submerged in a beaker full of deionized water. Said beaker was submerged in a Bransin Ultrasonics (Bransonic model CPX 3800) ultrasonic bath with frequency of 40kHz. The fibers were sonicated for 2, 4 and 6 hours. Fiber yarns were air dried and prepared for DMA testing. In order to maintain the fibers of the yarn together, a thin layer of epoxy glue was deposited at the ends of the yarns. Epoxy was let to set for 24 hours. **Table 2** offers information about the PPTA fibers used provided by the manufacturer in order to be compared with the results of the conducted experiments¹³.

Twaron Properties	
Density (g/cm ³)	1.44-1.45
Tensile Strength (GPa)	2.4-3.6
Tenacity (N/tex)	1.65-2.5
Modulus (GPa)	60-120
Elongation at break (%)	2.2-4.4
Moisture (wt%)	3.2-5
Decomposition (°C)	500

Table 2. Mechanical properties of Twaron (PPTA) fibers.

Another set of samples of woven PPTA were sonicated for the long creep test that will be described in **section 7.2.3**. These samples were sonicated for 2 hours in DI water and hexane.

7.2 Dynamic Mechanical Analysis

Experiments that measured the amount of creep with humidity were carried on a DMA Q800 from TA Instruments with a humidity chamber attached to it. Experiments were carried using a film-tension fixture.

7.2.1 Humidity ramp test

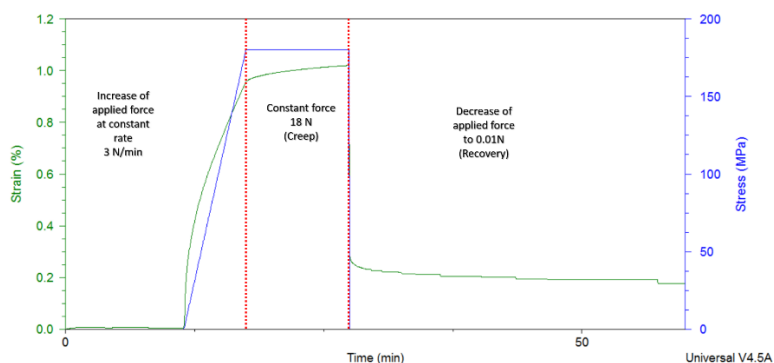


Figure 19. Segment of the humidity ramp test. For each percentage of relative humidity, the same steps are repeated.

Dynamic mechanical analysis was performed on neat and sonicated yarns. The DMA creep-humidity test consisted in a controlled force stress versus strain test (**figure 19**). Initial force was set at 0.01N and it was ramped up to 18N at a rate of 3N/min. The test consisted in measuring the response of the fibers to an applied force at a constant temperature and varying percentage of relative humidity. Once the applied force reached 18N it remained constant for 10 minutes to measure creep. After this creep period, the force was decreases to the original 0.01N. The applied stress was tested under 0, 50 and 80% relative humidity and then the humidity was decreased in the same steps but in reverse to 0% relative humidity. Temperature was kept constant at 30 and 60°C. **Figure 20** shows the humidity steps over the running time of the test.

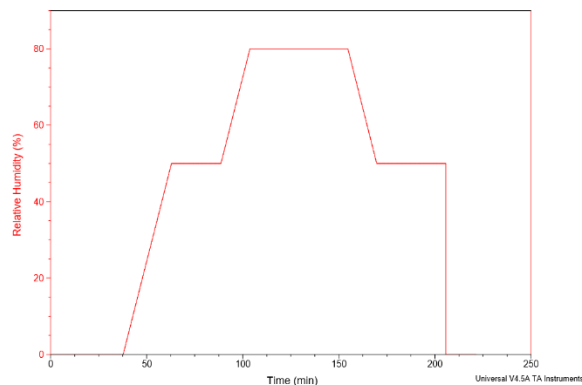


Figure 20. Relative humidity steps on the humidity ramp test. Temperature is kept constant through the test.

7.2.2 Cycle-humidity test

A similar tests to the one described in section 6.2.1 was made for neat and sonicated fiber yarns. The aim of this test was to induce fatigue on the fibers and measure their creep. The test consisted in two parts: (1) fatigue at 0% and (2) fatigue at 80%. Stress was applied with an initial force set at 0.01N and it was ramped up to 18N at a rate of 3N/min. Once the stress reached 18N it was held constant for 10 minutes and then decreased to 0.01N. This was repeated three times for both parts of the test, with a 10-minute interval (at 0.01N) between repetition. **Figure 21** illustrates the changes in humidity during this test. The tests were run isothermally (30°C and 60°C).

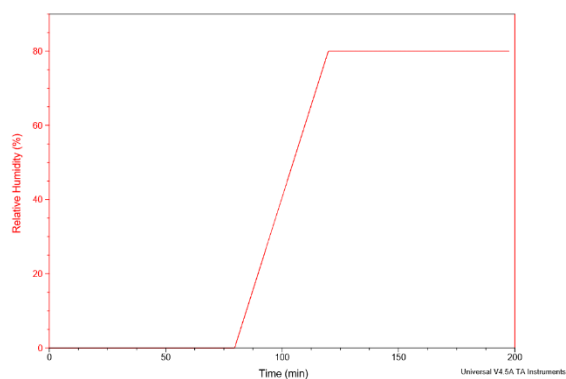


Figure 21. Relative humidity steps on the cycle-humidity test. Temperature is kept constant through the test.

7.2.3 Long Creep Test

To determine the formation of hydrogen bonding between PPTA crystallites and water, another test is carried, where the fibers are immersed in a non-polar solvent for same amount of time and conditions previously discussed. As said before, the ability of PPTA molecules to form hydrogen bonds, make possible the formation of water layers between the crystallites. Increasing the amount of water, increases the formation of layers which acts as a plasticizer and enables creep.

Hexane, a common non-polar solvent will be used to compare if the presence of water is in fact a factor that contributes to the increase of creep between the crystallites. **Table 3** includes information about this solvent. Obtaining data of the creep behavior of PPTA fibers that have been exposed to a non-polar solvent like hexane will validate or invalidate the hypothesis of the formation of water layers between PPTA crystallites.

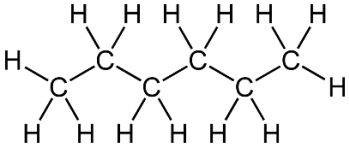
Hexane Chemical Properties				
Molecular Formula	Molecular Weight (g/mol)	Melting Point (°C)	Boiling Point (°C)	Molecular Structure
C ₆ H ₁₄	86.175	-95.35	68.73	

Table 3. Properties of the non-polar solvent, hexane.⁵⁵

Sample preparation for this test was described on **section 7.1**, where woven PPTA samples were sonicated in hexane and DI water for 2 hours respectively. After sonication, the woven material was dried for 30 minutes at 60°C to remove any excess solvent.

The DMA test consisted in applying the same constant force of 18N for two hours at 0% RH and isothermally at 30°C. The constant RH and temperature enables to have control over the amount of water in the fibers and only study the effects of water and sonication.

7.3 Humidity Chamber

A humidity chamber was built to humidify neat and sonicated fibers for 24 hours at a constant temperature (30°C) and humidity (~50% RH). **Figure 22** shows a schematic of the humidity chamber setup. This humidity chamber was used principally to prepare fiber samples which required to be longer for tensile testing to failure (see section 7.6) and to measure the amount of water uptake of the fibers through thermogravimetical analysis (see section 7.5).

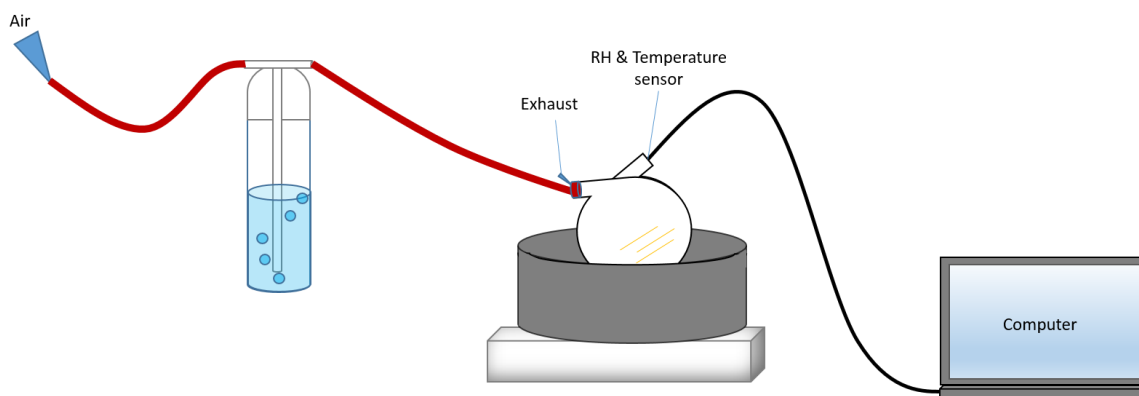


Figure 22. Sketch of the costume made humidity chamber.

7.4 Scanning Electron Microscopy (SEM)

Electron microscope images were taken using the XL40 FESEM from Philips. Images of the neat and sonicated fiber yarns were taken to detect any visual signs of degradation like fibrillation and kink bands. Also, fibers tested to failure were also examined.

7.5 Thermogravimetical analysis (TGA)

Humidified fiber samples (see section 7.3), were submitted to thermogravimetical analysis to detect the amount of water retained and any significant shifts on properties like the degradation temperature of neat and sonicated fibers. The test consisted of a temperature ramp from room temperature to 1000°C at a rate of 15°C/min.

7.6 Tensile Testing

Neat, sonicated and humidified fibers were tested to failure in a MTS Insight tensile tester (electromechanical-100kN standard length) with a load cell of 1000 N. A fiber fixture was used to test the fibers following the ASTM D 2256 standard. **Figure 23** shows the fixture used for this test. PPTA fibers with a gauge length of 432mm, 0.20mm of thickness and 0.50mm of width were tested. Tape was adhered to the ends of the fiber yarns to prevent slipping.



Figure 23. Fixture used for tensile testing.

CHAPTER 8: DATA

8.1 Humidity ramp test

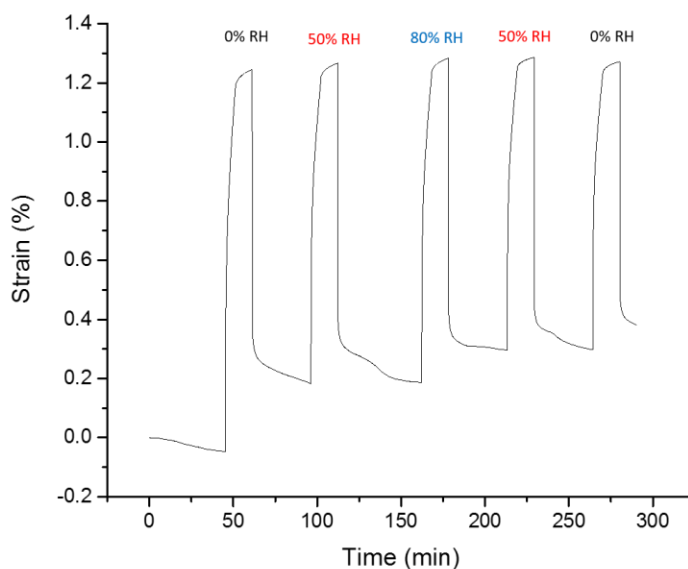


Figure 24. Complete humidity ramp test for neat PPTA fiber sample at 30°C.

Results from the humidity ramp test for one sample is showed in **figure 24**. The creep portion for each relative humidity are extracted from this data set. **Figures 25** and **26** show the creep response of neat PPTA fibers at 30°C and 60°C respectively. At 30°C the strain increases as the humidity increases. However, at 50% and 0%RH at recovery the final strain reached is almost the same as the acquired at 80%RH, with only a small decrease. (**figure 25**). A similar behavior is seen for neat fibers at 60°C at the initial 0% to 80% RH. Contrary to the neat fibers at 30°C, at 60°C the strain decreases drastically as the humidity is brought back to 0% RH (**figure 26**).

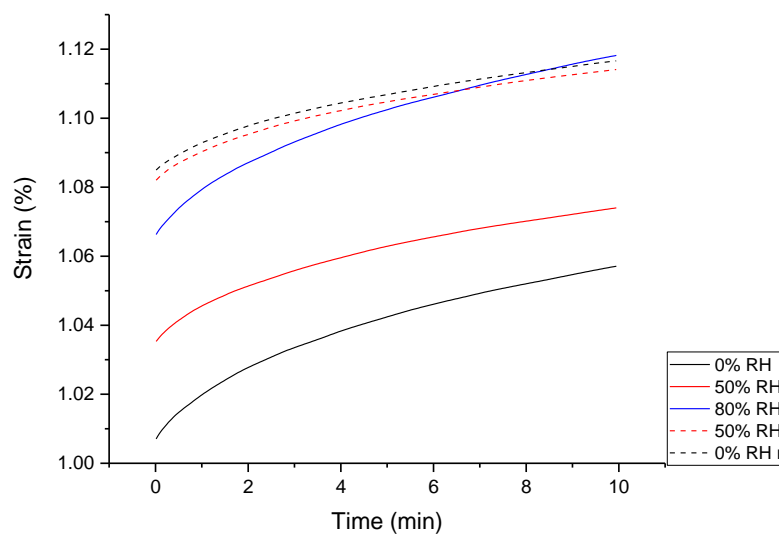


Figure 25. Humidity ramp test of neat PPTA fibers at 30°C.

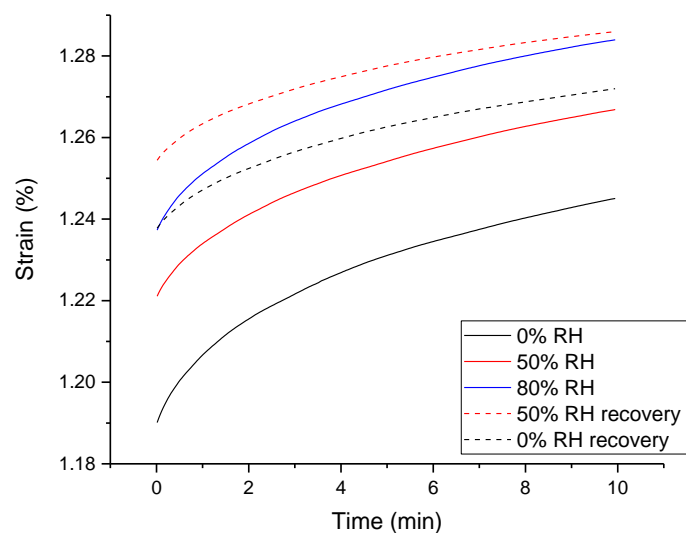


Figure 26. Humidity ramp test of neat PPTA fibers at 60°C.

All sonicated fibers tested exhibit the same general creep response as the neat fibers. At 30°C, the strain continues to increase as the humidity is brought back to 0% RH but at a smaller degree than the initial humidity steps. On the other hand, at 60°C, there is a “recovery” on the strain when the humidity is reaches the final 0%RH. This is true for both kinds of sonicated fiber- for 2 hours (**figures 27 and 28**) and 6 hours (**figures 29 and 30**). The reduction in the strain percent implies that there is more resistance to deformation.

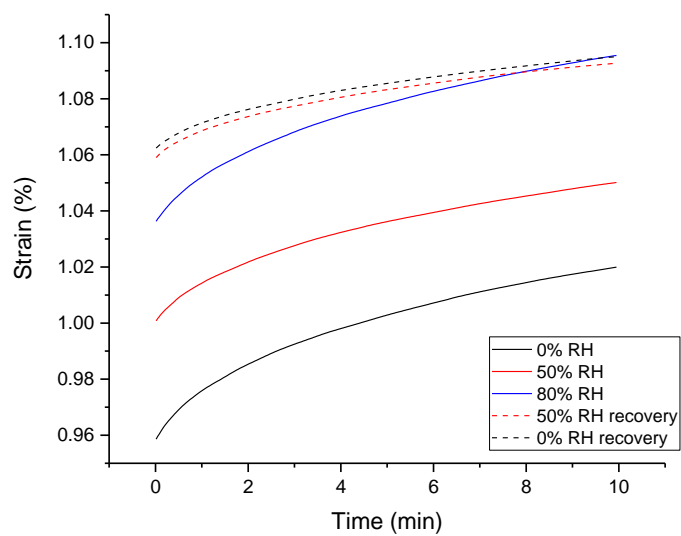


Figure 27. Humidity ramp test of PPTA fibers sonicated for 2 hours at 30°C.

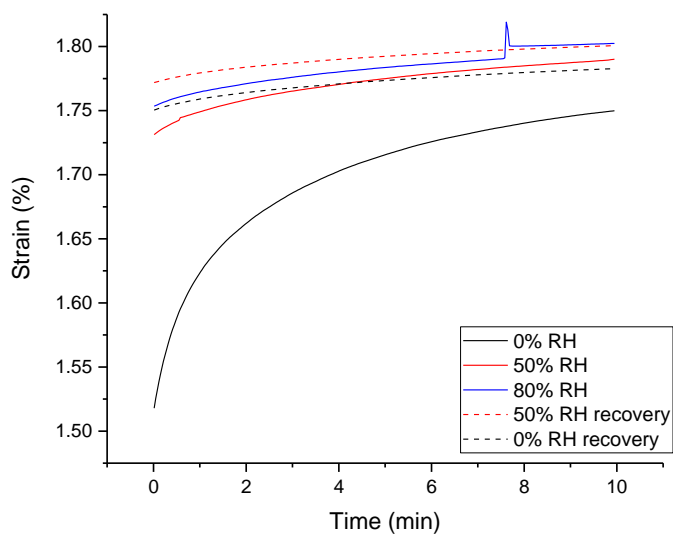


Figure 28. Humidity ramp test of PPTA fibers sonicated for 2 hours at 60°C.

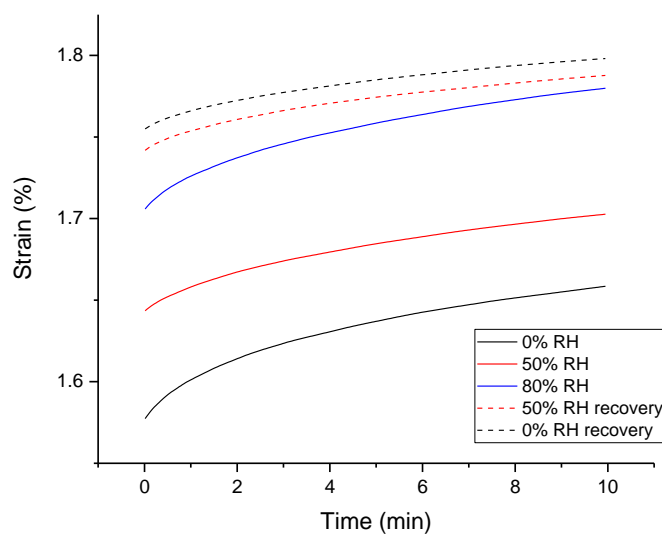


Figure 29. Humidity ramp test of PPTA fibers sonicated for 6 hours at 30°C.

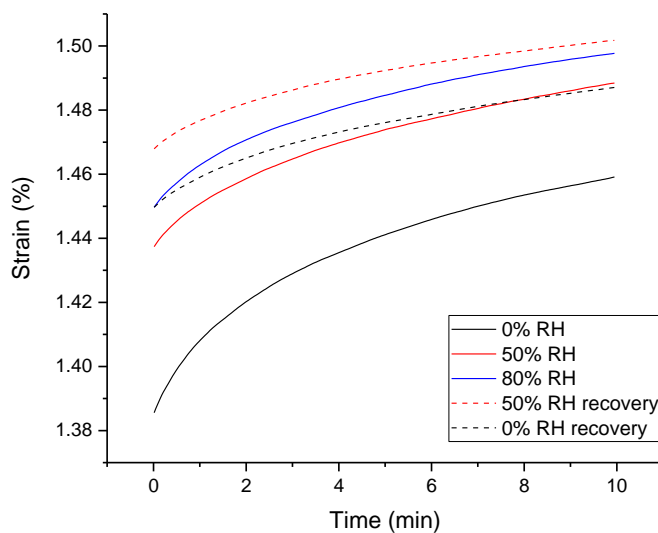


Figure 30. Humidity ramp test of PPTA fibers sonicated for 6 hours at 60°C.

One important factor to consider in these tests is time and the systematic restrictions from the DMA machine. In order to reach a certain percentage of relative humidity, the system has to undergo an isothermal step until it reaches the desired humidity. The rate at which the machine reaches the humidity is 2 %RH per minute. Therefore, in order to reach 80 %

RH, the system has to stay on an isothermal step for 40 minutes. Once at the desired %RH, the following step is a 10-minute creep stage, where the constant force is 18N. This means that the fibers have more time to respond to the humidity until it reaches the 80 % RH.

To understand the degree of strain at the end of the experiment, the strain history of the samples must be considered. As an approach to understand the overall effect of water adsorption, temperature and amount of sonication, a comparison of the values of the strain difference of all the fibers was made. The method used to calculate each data point is explained in section 6.3. This method correlates the final strain percent at each humidity with the initial strain at 0%RH. **Figure 31** is a plot of these percent differences.

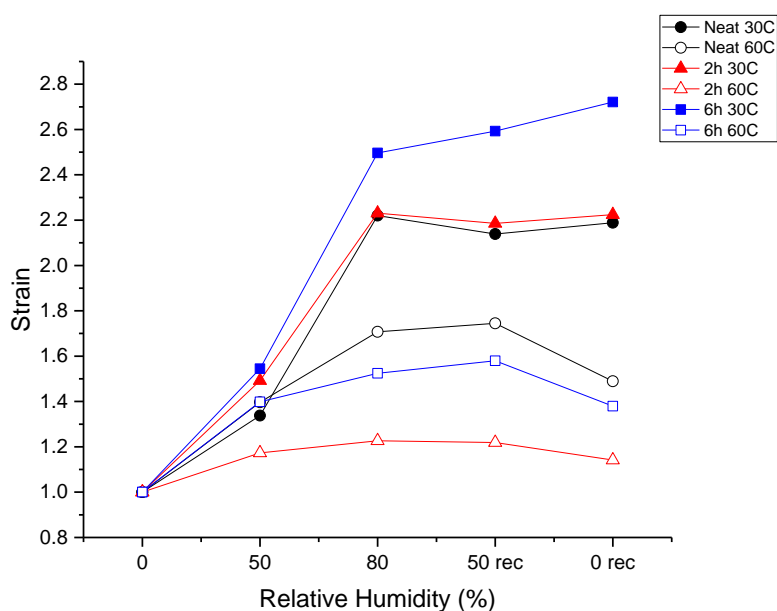


Figure 31. Strain percent difference under each condition related to the initial strain

Notice that **figure 31** offers a clearer view of the differences between the behavior of the fibers at 30°C and 60°C. Within each temperature the trend is the same for both neat and sonicated fibers. At 30°C (plots with square symbols), show an increase in the strain as the humidity increases. Once it reaches 80%RH and the humidity proceeds to decrease, the amount of strain is almost constant for the neat fibers and those sonicated for 2 hours. Fibers sonicated for 6 hours show an increment in their strain as the humidity is brought

back to 0% RH. At this temperature, the fibers can adsorb more water. Therefore, the strain values are greater at 30°C than at 60°C.

On the other hand, at 60°C the strains are lower and the overall trend is different. As humidity increases there is more strain, but once the humidity returns to 0%RH the amount of strain decreases. This could be due to the desorption of water which reduces the amount of water layers between the crystallites and induce stronger hydrogen bonding.

8.2 Cycle-humidity test

As described on section 7.2.2, the cycle-humidity test consisted in detecting the amount of creep after loading and unloading the sample yarns at 0% RH and 80%RH. **Figure 32-34** show the strain percentage neat and sonicated fibers undergo at 30°C. The results show that the amount of strain increases with humidity and also after every cycle.

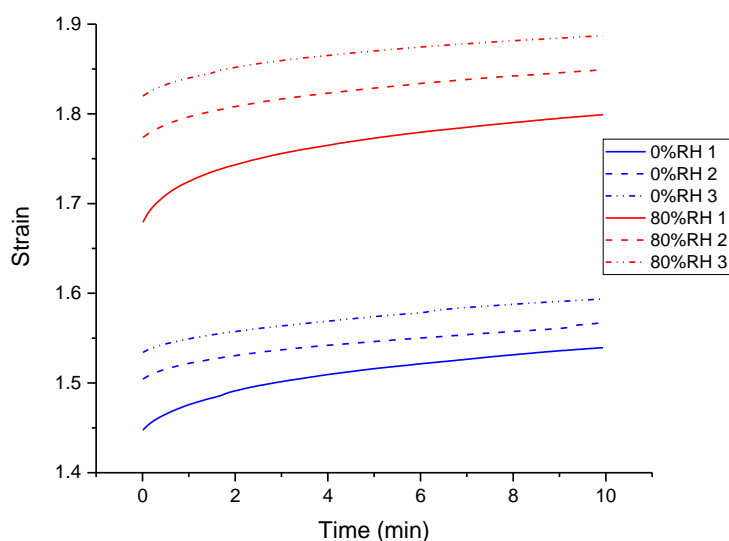


Figure 32. Cycle-humidity test for neat PPTA fibers at 30°C.

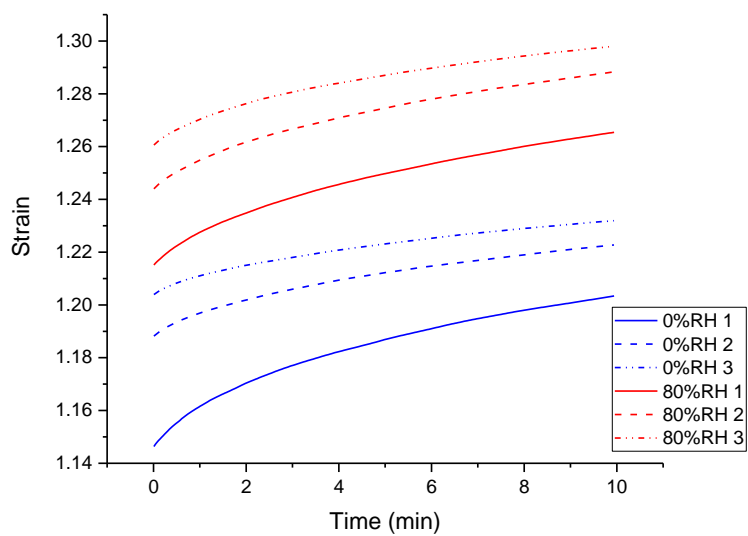


Figure 33. Cycle-humidity test for PPTA fibers sonicated for 2 hours.

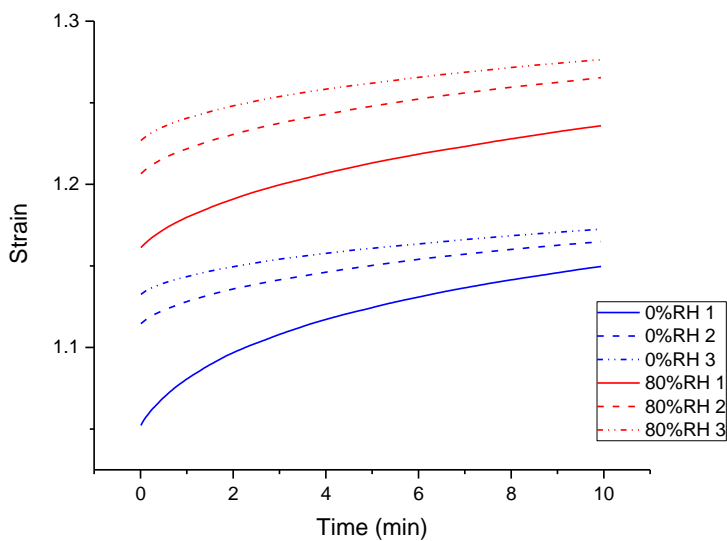


Figure 34. Cycle-humidity test for PPTA fibers sonicated for 6 hours.

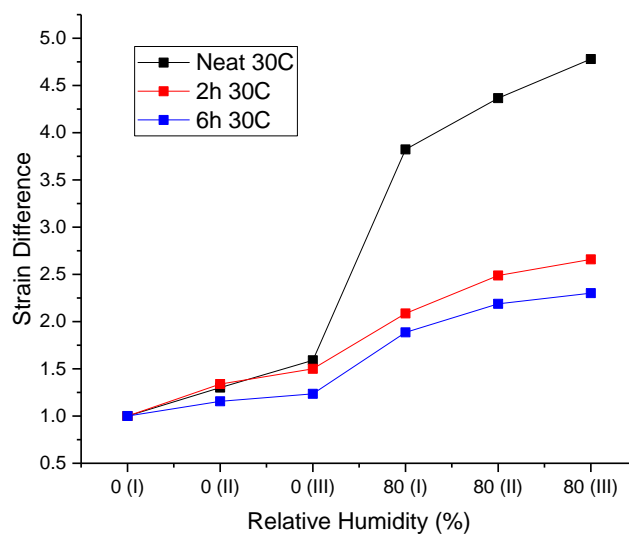


Figure 35. Comparison of the strain difference of neat and sonicated fibers at 30°C. This plot allows to compare the creep behavior of all the fibers after each cycle and their response to humidity.

Figure 35 compares the overall strain percent that the samples experience during fatigue at 0%RH and 80%RH. Three main observations in this graphs are the following: (1) strain is decreased with sonication, (2) strain increases with humidity, and (3) strain increases with each creep cycle. At 0% RH, small changes in the strain of the fibers are notable. In this stage, there is no moisture added, therefore the difference in the strain between the sonicated and neat yarns are attributed to the alteration of their crystalline structure due to sonication. This alteration prevents sliding.

A common factor among the fibers is that the strain increases drastically when moisture is added. Therefore, at 80% RH, strains are higher than at 0% RH. This level of humidity permits more adsorption of water molecules, creating more layers of water between the crystallites. Hence, greater strains are seen at 80%RH. It can be said that water acts as a “plasticizer”, allowing the chains to move. Neat PPTA fibers are more affected by moisture, while those sonicated for 6 hours are less affected. In other words, sonication hinders the amount of creep of PPTA fibers when exposed to humidity.

The third stipulated observation, acknowledges the creep history of the PPTA fibers. At any amount of humidity in the environment, the strain increases after each creep cycle.

Fatigue will always affect the fibers regardless the amount of water present and their previous condition or treatments because it creates changes in the structure, moving any dislocations. The difference on the response to fatigue between treated and neat fibers relays on how much fatigue affects the amount of strain. That said, results in **figure 35** show that sonication helps reduce the amount of creep contributed to fatigue.

8.3 Long Creep Test

Data obtained from the long creep tests discussed in **section 7.2.3** was fitted to the power law equation. The values of the fitting for each of the cases (neat fibers and fibers sonicated in water and hexane), are listed in **table 4**. These values where used to obtain the respective equations that will predict the creep behavior at longer periods of time.

Solvent	ε_0	m	n
Neat	1.68	0.22	0.12
Water	1.36	0.19	0.10
Hexane	1.30	0.15	0.11

Table 4. Values obtained from the fitting of the long creep test.

Figure 36 shows a plot of the creep behavior of the fibers under the different conditions for longer periods than the 2 hours on which the experiment was carried. For a clearer understanding of the effects of creep on neat and sonicated fibers on polar and non-polar solvents, **figure 37** offers the same information, however the strain is normalized and the time axis is set to a logarithmic scale.

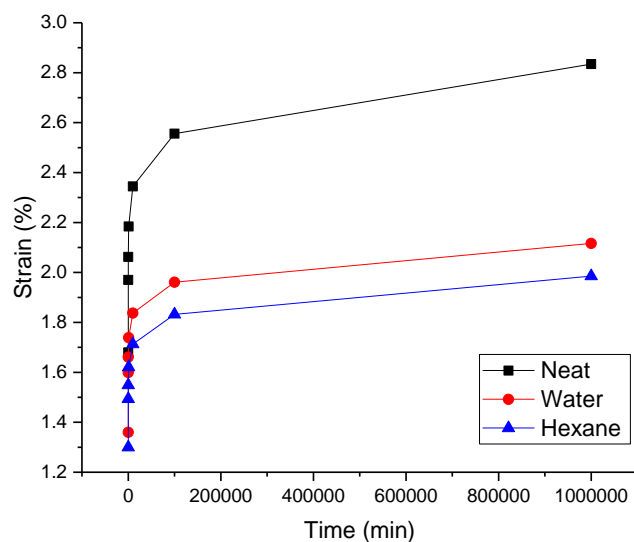


Figure 36. Prediction of the creep behavior of Neat and sonicated PPTA fibers on polar and non-polar solvents for 2 hours.

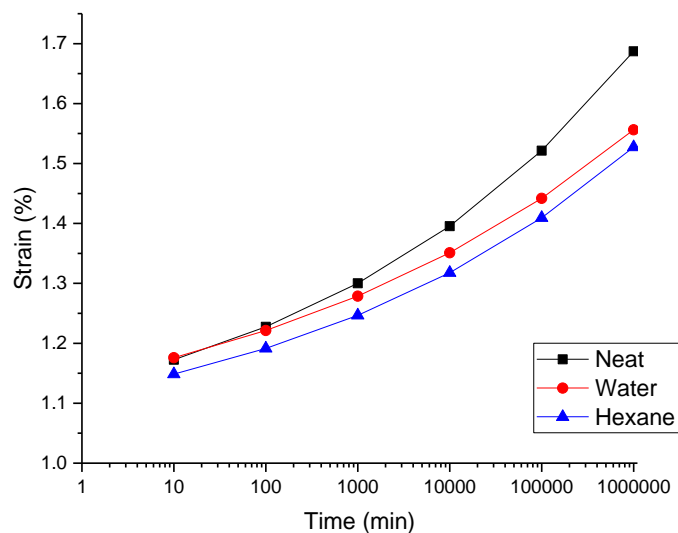


Figure 37. Prediction of the creep behavior of Neat and sonicated PPTA fibers on polar and non-polar solvents for 2 hours. Normalized strain and logarithmic time scale.

From the latter results it is noticed that neat fibers experience more creep than fiber sonicated for two hours in both water and hexane. This might indicate that sonication hinders the creep effect on the fibers. However, when the fibers sonicated on water are

compared to those sonicated on hexane, the former experience more creep than the latter. The formation of water layers between the PPTA crystallites allows more creep to take place. No hydrogen bonding is formed when fibers are submerged in a non-polar solvent, therefore, these fibers experience less creep.

In conclusion, sonication does hinder the creep effect on fibers, but the presence of water counteracts this effect, increasing the amount of creep but not in a higher rate than that of neat fibers.

8.4 SEM images

Cross sectional images were taken with the scanning electron microscope. The samples were set on epoxy and polished to obtain a flat surface to observe the cross sectional structure of the fibers. **Figure 38a** shows a group of fibers in a PPTA yarn. A closer look is taken in **figure 38b**, where the microstructure can be seen as well as some voids. Another detail that can be seen in this figure is the appearance of two fibers that seem to be attached to each other, which is commonly found in the rest of the sample. This could be as a result of the spinning process.

Figure 38c is a closer look at the microstructure of the fibers. These PPTA fibers are approximately 20 μm in diameter. However, the images obtained through this method might not resemble the real structure because in the polishing process heat is produced and abrasion is exerted on the microstructure. This is why the structure looks flattened in a direction. For this reason, other methods for the preparation of the samples to avoid damage are proposed in section 9.0. One of the proposed alternatives is to plasma etch the fibers in order to have a view of their microstructure in the lateral direction without cutting recurring to polishing that will cause additional harm to the sample.

Images of PPTA sonicated fibers were also obtained through scanning electron microscopy and show that there is not much of a difference between 2, 4 and 6 hours of sonication (**Figure 39**). Nevertheless, there are clear signs of fibrillation among the fibers.

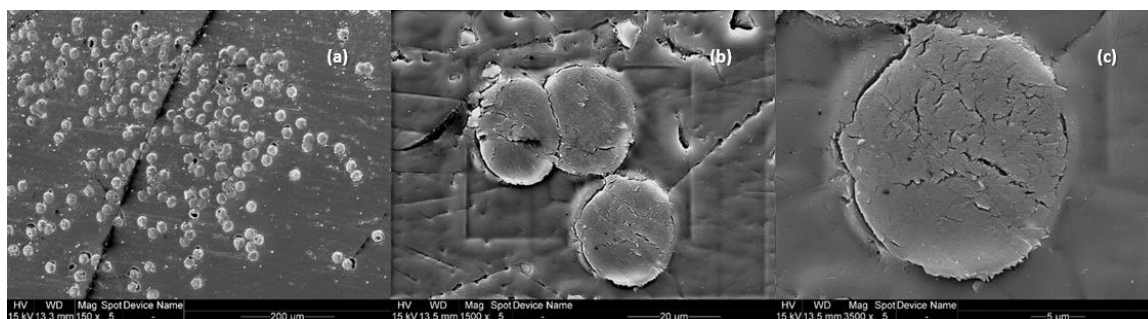


Figure 38. Cross sectional images of PPTA fibers in epoxy. (a) Cross sectional view of neat PPTA yarn. (b) Closer look of PPT fibers from the same yarn as in figure 36a, where some fibers are adhered to each other. (c) Cross sectional image of a single PPTA fiber.

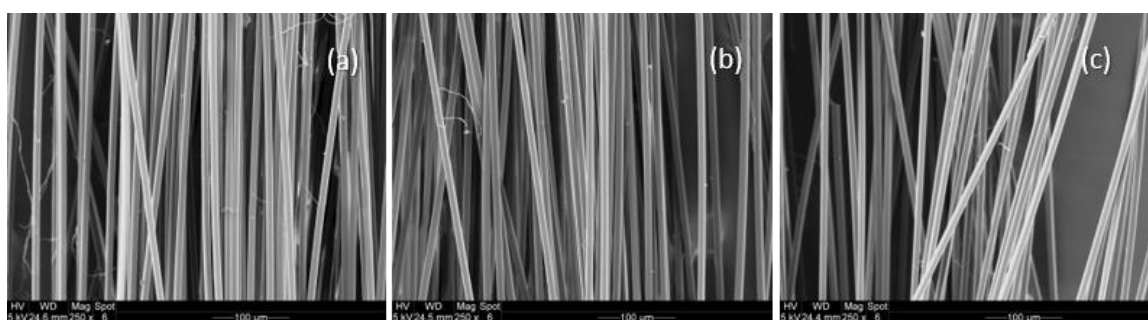


Figure 39. SEM images of PPTA fibers sonicated at (a) 2 hours, (b) 4 hours and (c) 6 hours. All images have a 100x magnitude.

A closer look reveals the presence of kink bands (see **Figure 40a**). Structure of fibers tested to failure are shown in **figures 40b and 40c**. In the latter evidence of fibrillar failure is observed.

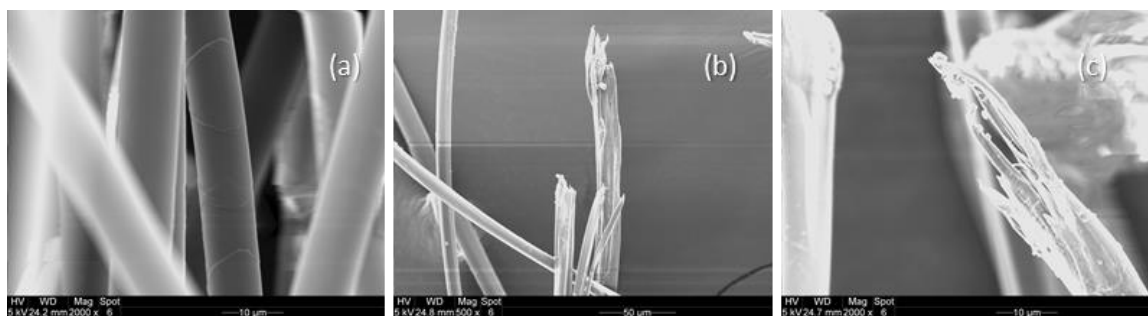


Figure 40. (a) Evidence of the presence of kink bands in sonicated PPTA fibers. Kink bands are a sign that the fibers experienced compression. 2000x magnitude. (b) Evidence of fibrillation fracture. 500x magnitude. (c) Closer look of the fibrillation in the fracture area of a fiber sonicated for 2 hours. 2000x magnitude

8.5 Thermogravimetical analysis (TGA)

Data obtained from the TGA is analyzed as explained in **figure 41**. This is a straight forward measurement of the amount of water that the fibers retain in terms of weight percent. According to the information provided by the manufacturer, Twaron PPTA fibers can have moisture uptake of 3.2-5 wt.% (see **table 2**). Neat and sonicated fibers are tested under the conditions mentioned in sections 7.3 and 7.5.

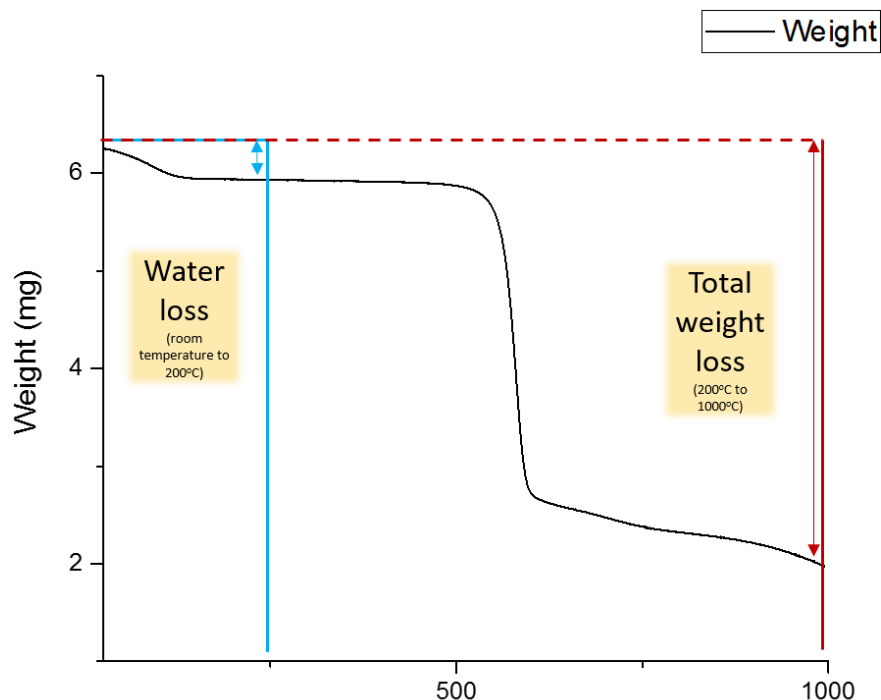


Figure 41. Example of how TGA data is analyzed. The x axis indicates the temperature. Change in weight is measured at 200 C to obtain the amount of water lost. This indicates the amount of water retained by the fibers. Results are reported as weight percent.

Results for the TGA analysis are plotted on **figure 42** Fibers sonicated for 2 hours retain less moisture than those sonicated for 6 hours. Therefore, the amount of moisture increases with sonication time. However, the amount of moisture decreases after 24 hours at 30°C and 50%RH. This could be for various reasons such as: evaporation of water and temperature gradient in the humidity chamber. The latter is due to the contact of the fibers to the bottom of the flask, which it is assumed that has a higher temperature than the rest of the round flask because it is in direct contact with the sand bath.

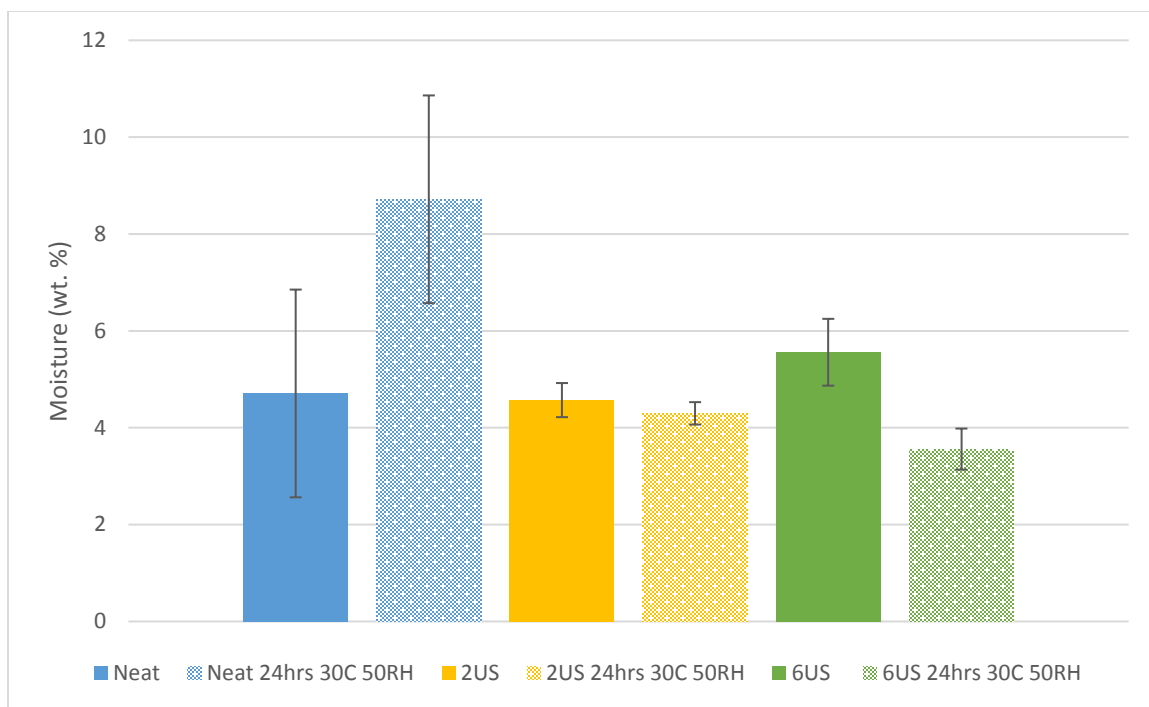


Figure 42. Moisture uptake of sonicated PPTA fibers after sonication and after 24 hours exposed to 30°C and 50% RH.

On the other hand, results show that neat PPTA fibers has an average moisture uptake similar to the fibers sonicated at 2 hours. Despite the trend seen among sonicated and sonicated-humidified fibers, where there is a reduction of the retained moisture after 24 hours, neat PPTA after 24 hours in the humidity chamber has a higher amount of moisture than the rest, including the completely neat fibers. These results also might be an indication of changes in the crystalline structure of the fibers that cause greater water uptake.

8.6 Tensile Testing

Results of the discussed test in section 7.6 are shown on **figure 43**, where the modulus of neat, and sonicated PPTA fibers were tested to failure. These also include the testing of humidified fibers for 24 hours. Neat PPTA fibers have an average modulus of 105 GPa, however, after 24 hours of humidification the modulus decreases to 93 GPa. A greater decrease on the modulus is obtained after 2 hours of sonification. The effect of humidity after 24 hours for fibers sonicated for two hours does not have a dramatic effect on the modulus. As sonication is continued for 6 hours, modulus is slightly increased when

compared to the fibers sonicated for 2 hours. Nevertheless, humidification for 24 hours does decrease the modulus, having a similar behavior as the neat PPTA fibers. Overall, there is not a significant change in the modulus.

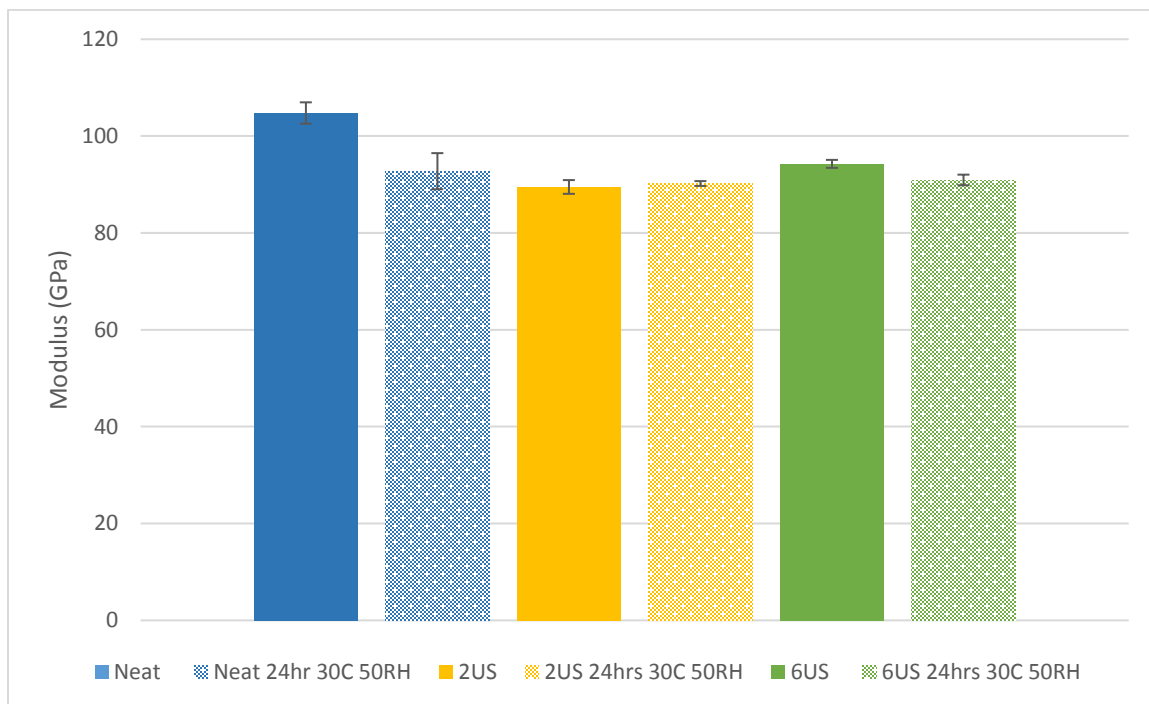


Figure 43. Elastic modulus of neat and sonicated fibers after sonication and 24 hours in the humidity chamber at 30°C and 50% RH.

Although no significant changes in the modulus are detected, the peak load of the fibers is affected by sonication and humidity. The peak load of the fibers is the load at which the fibers break, also known as the ultimate tensile strength (UTS). **Figure 44** shows the results of the peak load of neat and sonicated fibers. The peak load of the neat fibers is the same even after 24 hours of humidification. As the fibers are sonicated, the peak load increases, which can be attributed to changes in the crystalline structure and the amount of water between the crystallites. In section 6.3, we discussed that water molecules enter the fibers and form layers that are attached to the crystallites by hydrogen bonding. A monolayer of water may increase the strength between the crystallites, preventing their mobilization. It can be assumed that as sonication time increases, more areas where the water layers can form are created. Hence, the peak load increases with sonication.

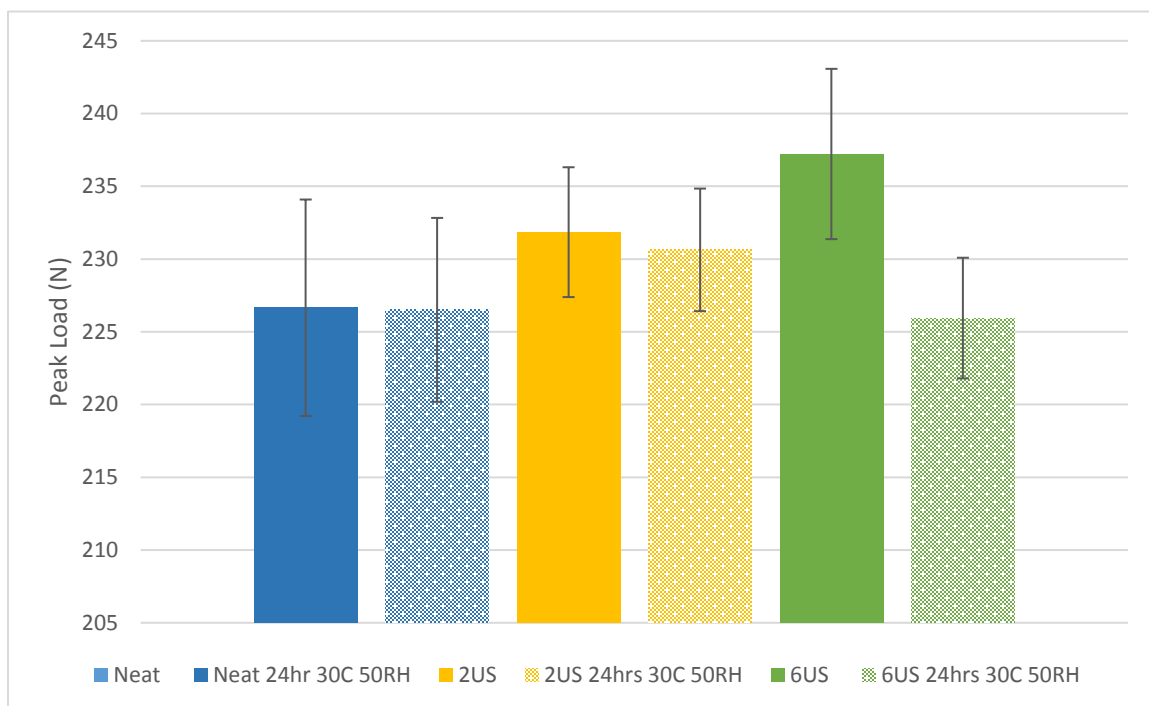


Figure 44. Peak load of neat and sonicated fibers after sonication and 24 hours in the humidity chamber at 30°C and 50% RH.

Comparing the results of neat and sonicated fibers to their humidified counterparts, a decrease in the peak load is detected. As mentioned before, sonication may produce more dislocations or changes in the crystalline structure of the fibers, permitting the adsorption of more water molecules. However, if the amount of water increases (more layers of water are formed), the strength of bonds between the water molecules and the crystallites decrease. This is why after 24 hours in the humidity chamber there is a decrease in the peak load for sonicated fibers. Fibers sonicated for 6 hours and exposed to humidity for 24 hours have a more dramatic decrease in the peak load.

CHAPTER 9: CONCLUSIONS AND FUTURE WORK

Results of this project show that both sonication and humidity affect the creep behavior of PPTA fibers. Moreover, the dynamic mechanical analysis is a viable method to detect small changes in the strain of PPTA fibers. This technique allows the measurement of the amount of creep in the fibers while controlling the temperature and humidity in the environment. Therefore, the creep detected in this study is the immediate response of this material to the changes in these factors. These results are related to the early stage of creep (where the strain rate decreases), more known as the primary creep stage, and can help predict the failure of these fibers that have been exposed to these factors for a longer amount of time.

DMA results are correlated to the results obtained through tensile testing to failure. Sonicated fibers that went through various load and unloading cycles show lower amount of creep (lower values of strain) when compared to neat fibers (see section 8.2). This is a trend also observed in the results of the tensile test, where sonicated fibers showed higher peak load than neat fibers.

Humidity plays an important role on the property loss resulting from degradation of PPTA fibers. The amount of water retained between the crystallites determines the creep response of the fibers. If there is more water, more strain and therefore more creep is experienced. Moreover, fibers that have higher amount of water tend to fail at lower loads. This explains why sonicated fibers that were humidified for 24 hours in the humidity chamber at 30°C show failure at lower applied loads.

Although other studies have concluded that sonication prevents UV degradation of PPTA fibers and it might seem beneficial, exposure to UV radiation is not the only factor that causes the loss of performance. Humidity is a very common factor that contributes to the degradation of polymeric materials such as fibers, and can be provided by sweat, the storage environment, and even the weather. The magnitude of the effects contributed by humidity increased with time and the ability of the material to retain moisture.

One of the reasons why sonication seems to increase the strength of the fibers can be the alteration of the crystalline structure. These changes act as an obstacle for the movement of dislocations and together with the small amount of water that might be trapped by

hydrogen bonding, strengthens the material. However, as the humidity increases more water is able to get trapped between the crystallites on sonicated and have the contrary effect. Still, sonication can hinder the effects of fatigue (as seen in the results of the cycle-humidity DMA test), reducing the amount of creep, but the presence of high amounts of moisture increases the amount of strain.

Moreover, the formation of water layers between PPTA crystallites is confirmed when compared to the effects of a non-polar solvent like hexane. PPTA fibers sonicated in hexane show lower creep at longer times than fibers exposed to water. Hence, water layers and hydrogen bonding form between PPTA crystallites.

At higher temperatures like 60°C, desorption can take place in a greater magnitude than at temperatures closer to room temperature (30°C). Results on the humidity ramp DMA test at 60°C confirm this conclusion, where the fibers tested at 30°C show a higher amount of creep. The former shows a decrease in the amount of creep when the humidity is lowered back to 0%RH. This can be attributed to the removal of water between the crystallites, hence may be occurring. Overall, fibers tested at 60°C show a lower strain difference because they experience a higher apparent temperature. The apparent temperature refers to the temperature that is perceived as a result of the combination of the actual temperature and the percentage of relative humidity. This temperature increases with relative humidity. Therefore, the samples at 60°C may behave as if they were on an environment with higher temperatures. That said, at higher temperatures neat fibers show more strain than those sonicated, thus, sonication seems to hinder the effects of creep at these conditions.

To confirm and obtain a quantitative measurement of the effects of sonication in the crystalline structure, techniques such as small angle x-ray diffraction may be used in the future. However, to study the effects of humidity on the crystalline structure can be more complex. DMA results show that really small changes in the temperature and relative humidity alter the strain of the fibers. Therefore, an experimental setup should be developed to study these measurements in-situ and x-ray diffraction data is acquired.

Likewise, another characterization technique can be used to study the effects of humidity and temperature at early degradation stages. It is a non-destructive characterization method known as positron annihilation lifetime spectroscopy (PALS). PALS consists in emitting

positron from a radioactive source (Na^{22}) that is in contact with the material. The positrons diffuse through the material and occupy areas of low electron density like the free volume in polymers. When a positron annihilates with an electron a positronium is formed and emitted. The lifetime of a positronium is related to the size of the free volume and the intensity is related to the amount of free volume. The result of the spectroscopy is a lifetime distribution.

Although PPTA fibers are highly crystalline and the free volume is found the amorphous areas, changes in the small quantity of free volume and in the defects of the polymer can be detected with PALS. Through this method early signs of degradation may be detected and can complement the information obtained in this study. Neat and fibers sonicated for 2 and 6 hours will be tested with PALS for 24 hours. To study the effects of humidity as the experiment is taking place, a humidity chamber will be attached to the PALS setup. Data for the latter experiment will also be acquired for 24 hours.

More studies can be developed based on these data. Further and more thorough SEM images of the structure of the PPTA fibers can be obtained by submitting the sample to plasma etching. Also, studies on the effects of sonication under different media- like water with a pH range of 3 to 11- can be carried out and used to mimic the effects of wear and exposure to human sweat.

Long term studies of the hydrothermal degradation of PPTA fibers will be performed. These will consist in aging the fibers that are submerged in different water solutions that vary in their pH and exposed to a constant temperature for 6 weeks. Data will be collected with characterization methods such as DMA, tensile testing, TGA, FTIR, PALS and SEM to gather as much information of the chemical and mechanical changes through the degradation process. This study will be extended to other high performance fibers such as PBO, UHMWPE among others.

REFERENCES

- (1) Materials, F. Physical Properties of Fillers and Filled Materials. *c*, 241–303.
- (2) Mather, R. R.; Wardman, R. H. *The Chemistry of Textile Fibers*; RSC Publishing, 2011.
- (3) Strobl, G. R. Chapter 10: Deformation, Yielding and Fracture. In *The Physics of Polymers*; 2007.
- (4) Piazza, R. *Soft Matter: The Stuff that Dreams are Made of*; Springer: Milan, Italy, 2010.
- (5) Buschow, K.H. Jürgen Cahn, Robert W. Flemings, Merton C. Ilschner, Bernhard Kramer, Edward J. Mahajan, S. *Encyclopedia of Material-Science and Technology*; Elsevier, 2001; Vol. 1–11.
- (6) Ahmed, D.; Hongpeng, Z.; Haijuan, K.; Jing, L.; Yu, M.; Muhuo, Y. Microstructural Developments of Poly (p-phenylene terephthalamide) Fibers During Heat Treatment Process : A Review. *Mater. Research* **2014**, *17* (5), 1180–1200 DOI: 10.1590/1516-1439.250313.
- (7) Wilusz, E. *Military Textiles*; Woodhead Publishing Limited, 2008.
- (8) Dobb, M. G.; Johnson, D. J.; Majeed, A.; Saville, B. P. Microvoids in aramid-type fibrous polymers. *Polymer* **1979**, *20*, 1284–1288 DOI: 10.1016/0032-3861(79)90157-5.
- (9) Committee on Opportunities in Protection Materials Science and Technology for Future Army Applications, and National Research Council. Opportunities in Protection Materials Science and Technology for Future Army Applications. Washington, DC, USA: National. **2016**, No. March.

- (10) Fukuda, M.; Ochi, M.; Miyagawa, M.; Kawai, H. Moisture Sorption Mechanism of Aromatic Polyamide Fibers: Stoichiometry of the Water Sorbed in Poly(paraphenylene Terephthalamide) Fibers. *Text. Res. J.* **1991**, *61* (11), 668–680 DOI: 10.1177/004051759106101107.
- (11) Marissen, R.; Duurkoop, D.; Hoefnagels, H.; Bergsma, O. K. Creep forming of high strength polyethylene fiber prepregs for the production of ballistic protection helmets. *Compos. Sci. Technol.* **2010**, *70* (7), 1184–1188 DOI: 10.1016/j.compscitech.2010.03.003.
- (12) Li, C. S.; Zhan, M. S.; Huang, X. C.; Zhou, H. Degradation behavior of ultra-high molecular weight polyethylene fibers under artificial accelerated weathering. *Polym. Test.* **2012**, *31* (7), 938–943 DOI: 10.1016/j.polymertesting.2012.06.009.
- (13) Twaron – a versatile high-performance fiber.
- (14) Kitagawa, T.; Yabuki, K.; Young, R. . An investigation into the relationship between processing, structure and properties for high-modulus PBO fibres. Part 1. Raman band shifts and broadening in tension and compression. *Polymer* **2001**, *42* (5), 2101–2112 DOI: 10.1016/S0032-3861(00)00571-1.
- (15) Park, E. S.; Sieber, J.; Guttman, C.; Rice, K.; Flynn, K.; Watson, S.; Holmes, G. Methodology for detecting residual phosphoric acid in polybenzoxazole fibers. *Anal. Chem.* **2009**, *81* (23), 9607–9617 DOI: 10.1021/ac901602x.
- (16) Forster, A. L.; Pintus, P.; Messin, G. H. R.; Riley, M. a.; Petit, S.; Rossiter, W.; Chin, J.; Rice, K. D. Hydrolytic stability of polybenzobisoxazole and polyterephthalamide body armor. *Polym. Degrad. Stab.* **2011**, *96* (2), 247–254 DOI: 10.1016/j.polymdegradstab.2010.10.004.
- (17) Gabra, V.; Hartzler, J. D.; Lee, K. S.; Rodini, D. J.; Yang, H. H. *Handbook of Fiber Chemistry*; Taylor & Francis Group, 2006.
- (18) Wallenberger, F. T.; Industries, P. P. G. Introduction to Reinforcing Fibers. **2001**, *21*, 50–53 DOI: 10.1361/asmhba0003352.

- (19) Rebouillat, S. *High Performance Fibres*; Hearle, J. W. S., Ed.; Woodhead Publishing Limited: Cambridge, England, 2001.
- (20) Young, R. J.; Lovell, P. A. *Introduction to Polymers*, 3rd ed.; CRC Press: Boca Raton, FL, 2011.
- (21) Sawyer, L. C.; Chen, R. T.; Jamieson, M. G.; Musselman, I. H.; Russell, P. E. The fibrillar hierarchy in liquid crystalline polymers. *J. Mater. Sci.* **1993**, 28 (1), 225–238 DOI: 10.1007/BF00349055.
- (22) Yang, H. H. *Kevlar Aramid Fiber*; John Wiley & Sons, Inc., 1992.
- (23) Yang, H. H. Aramid fibers. In *Comprehensive Composite Materials*; 2000; pp 199–229.
- (24) Chatzi, E. G.; Koenig, J. L. Morphology and structure of Kevlar fibers: a review. *Polym. Plast. Technol. Eng.* **1987**, 26 (3–4), 229–270 DOI: 10.1080/03602558708071938.
- (25) Li, L. S.; Allard, L. F.; Bigelow, W. C. On the morphology of aromatic polyamide fibers (Kevlar, Kevlar-49, and PRD-49). *J. Macromol. Sci. Part B* **1983**, 22 (May 2014), 269–290 DOI: 10.1080/00222348308215504.
- (26) Dobb, M. G.; Johnson, D. J.; Saville, B. P. Supramolecular structure of a high-modulus polyaromatic fiber (Kevlar 49). *J. Polym. Sci. Polym. Phys. Ed.* **1977**, 15, 2201–2211 DOI: 10.1002/pol.1977.180151212.
- (27) Morgan, R. J.; Pruneda, C.; Steele, W. J. The Relationship between the Physical Structure and the Microscopic Deformation and Failure Processes of Poly(p-Phenylene Terephthalamide) Fibers. *J. Polym. Sci. Polym. Phys. Ed.* **1983**, 21, 1757–1783 DOI: 10.1002/pol.1983.180210913.
- (28) Kelen, T. *Polymer Degradation*; Van Nostrand Reinhold Company, 1983.
- (29) Forster, A. L. Long Term Stability and Implications for Performance of High Strength Fibers Used in Body Armor, University of Maryland, 2012.

- (30) Hearle, J. W. S. *Fracture of highly oriented, chain-extended polymer fibres*; Elsevier Science Ltd., 2002.
- (31) Menard, K. P. An Introduction to Dynamic Mechanical Analysis. *Dyn. Mech. Anal. A Pract. Introd.* **1997**, No. approximately 1958, 7–22.
- (32) Barrett, C. R.; Nix, W. D.; Tetelman, A. S. *The Principles of Engineering Materials*; Prentice Hall: New Jersey, 1973.
- (33) Moosbrugger, C.; International, A. S. M. Representation of Stress-Strain Behavior. No. Eq 3, 1–19.
- (34) Callister, W. D. *Materials Science and Engineering : An Introduction*; John Wiley & Sons, Inc., 2007.
- (35) Abu Obaid, A.; Deitzel, J. M.; Gillespie, J. W.; Zheng, J. Q. The effects of environmental conditioning on tensile properties of high performance aramid fibers at near-ambient temperatures. *J. Compos. Mater.* **2011**, 45 (11), 1217–1231 DOI: 10.1177/0021998310381436.
- (36) Liu, X.; Yu, W. Evaluating the thermal stability of high performance fibers by TGA. *J. Appl. Polym. Sci.* **2006**, 99 (3), 937–944 DOI: 10.1002/app.22305.
- (37) Perepelkin, K. E.; Andreeva, I. V; Pakshver, E. A. Thermal Characteristic of para-Aramid Fibers. **2003**, 35 (4), 22–26.
- (38) Kim, J. H.; Brandenburg, N.; McDonough, W.; Blair, W.; Holmes, G. a. A Device for Mechanically Folding Yarns and Woven Fabrics of Ballistic Fibers. *J. Appl. Mech.* **2008**, 75 (1), 15001 DOI: 10.1115/1.2755131.
- (39) Holmes, G. A.; Kim, J.-H.; Ho, D. L.; McDonough, W. G. The Role of Folding in the Degradation of Ballistic Fibers. *Polym. Compos.* **2010**, 879–886 DOI: 10.1002/pc.
- (40) Mcluckey, S. A. Chapter 24. *Proteins* 492, 664–700 DOI: 10.1007/978-1-59745-493-3.

- (41) Masselin, I.; Chasseray, X.; Durand-Bourlier, L.; Lainé, J. M.; Syzaret, P. Y.; Lemordant, D. Effect of sonication on polymeric membranes. *J. Memb. Sci.* **2001**, *181* (2), 213–220 DOI: 10.1016/S0376-7388(00)00534-2.
- (42) Renouard, S.; Hano, C.; Doussot, J.; Blondeau, J. P.; Lainé, E. Characterization of ultrasonic impact on coir, flax and hemp fibers. *Mater. Lett.* **2014**, *129*, 137–141 DOI: 10.1016/j.matlet.2014.05.018.
- (43) Tomljenovic, a.; Unko, R. Reducing Fibrillation Tendency of Man-made Cellulose Fibres Employing Ultrasound Treatment. *J. Text. Inst.* **2004**, *95* (1), 327–339 DOI: 10.1533/joti.2003.0059.
- (44) Mohod, A. V.; Gogate, P. R. Ultrasonic degradation of polymers: Effect of operating parameters and intensification using additives for carboxymethyl cellulose (CMC) and polyvinyl alcohol (PVA). *Ultrason. Sonochem.* **2011**, *18* (3), 727–734 DOI: 10.1016/j.ultsonch.2010.11.002.
- (45) Price, G. J.; Smith, P. F. Ultrasonic degradation of polymer solutions. 1. Polystyrene revisited. *Polym. Int.* **1991**, *24* (3), 159–164 DOI: 10.1002/pi.4990240306.
- (46) Andrassy, M.; Pezelj, E. Reduction of Aging Tendency in p-Aramide Fibers. **1999**, 2340–2345.
- (47) Iyer, R.V. , Vijayan, K. Ultrasonic Agitation of Kevlar Fibres. *Curr. Sci.* **1996**, *71* (5), 398–400.
- (48) Mooney, D. A.; MacElroy, J. M. D. Differential water sorption studies on Kevlar 49 and as-polymerised poly (p-phenylene terephthalamide): Adsorption and desorption isotherms. *Chem. Eng. Sci.* **2004**, *59* (11), 2159–2170 DOI: 10.1016/j.ces.2004.02.011.
- (49) Division, M. S. Moisture uptake by Kevlar fibres. **1993**, *12*, 60–62.

- (50) Mooney, D. A.; Macelroy, J. M. D. Differential water sorption studies on Kevlar 49 and as-polymerized poly(p-phenylene terephthalamide): Determination of water transport properties. *Langmuir* **2007**, *23* (23), 11804–11811 DOI: 10.1021/la7017538.
- (51) Brinson, H. F.; Brinson, L. C. *Polymer Engineering Science and Viscoelasticity*; 2015.
- (52) Wang, J. Z.; Dillard, D. A.; Ward, T. C. Temperature and stress effects in the creep of aramid fibers under transient moisture conditions and discussions on the mechanisms. *J. Polym. Sci. Part B Polym. Phys.* **1992**, *30* (12), 1391–1400 DOI: 10.1002/polb.1992.090301210.
- (53) Argon, A. S. *The Physics of Deformation and Fractures of Polymers*; Cambridge Solid State Science Series, 2013.
- (54) Hearle, J. W. S. Forms of fibre fracture. In *FIBER FRACTURE*; Elsevier Science Ltd., 2002; pp 57–71.
- (55) Group, T. and F. Hexane-Properties of Organic Compounds.